

# Real-time renormalization group and cutoff scales in nonequilibrium applied to an arbitrary quantum dot in the Coulomb blockade regime

Thomas Korb,<sup>1</sup> Frank Reininghaus,<sup>1</sup> Herbert Schoeller,<sup>1</sup> and Jürgen König<sup>2</sup>

<sup>1</sup>*Institut für Theoretische Physik, Lehrstuhl A, RWTH Aachen, 52056 Aachen, Germany*

<sup>2</sup>*Institut für Theoretische Physik III, Ruhr-Universität Bochum, 44780 Bochum, Germany*

(Dated: October 25, 2018)

We apply the real-time renormalization group (RG) in nonequilibrium to an arbitrary quantum dot in the Coulomb blockade regime. Within one-loop RG-equations, we include self-consistently the kernel governing the dynamics of the reduced density matrix of the dot. As a result, we find that relaxation and dephasing rates generically cut off the RG flow. In addition, we include all other cutoff scales defined by temperature, energy excitations, frequency, and voltage. We apply the formalism to transport through single molecular magnets, realized by the fully anisotropic Kondo model (with three different exchange couplings  $J_x$ ,  $J_y$ , and  $J_z$ ) in a magnetic field  $h_z$ . We calculate the differential conductance as function of bias voltage  $V$  and discuss a quantum phase transition which can be tuned by changing the sign of  $J_x J_y J_z$  via the anisotropy parameters. Finally, we calculate the noise  $S(\Omega)$  at finite frequency  $\Omega$  for the isotropic Kondo model and find that the dephasing rate determines the height of the shoulders in  $dS(\Omega)/d\Omega$  near  $\Omega = V$ .

PACS numbers: 73.63.Nm, 05.10.Cc, 72.10.Bg

## I. INTRODUCTION

A fundamental issue of recent interest is the development of renormalization group (RG) methods in nonequilibrium.<sup>1,2,3,4,5,6,7,8,9</sup> Besides the discovery of new power law exponents for the conductance induced by nonequilibrium occupation probabilities,<sup>8</sup> an interesting question was raised whether voltage-induced decay rates provide additional cutoffs of the RG flow.<sup>5,10</sup> In this context, the nonequilibrium Kondo model has been discussed, which can be realized by a single-level quantum dot (QD) in the Coulomb-blockade (CB) regime coupled via spin exchange processes  $J_{\alpha\alpha'}$  to two reservoirs  $\alpha = L, R$ . In the isotropic case and above all cutoff scales, the exchange couplings  $J = J_{\alpha\alpha'}$  are all the same and are enhanced by reducing the band width  $\Lambda$  of the reservoirs according to the poor man's scaling equation  $\frac{dJ}{d\ell} = 2J^2$ ,<sup>11</sup> with  $l = \ln(\Lambda_0/\Lambda)$  ( $\Lambda_0$  denotes the initial band width). The enhanced screening of the dot spin leads to the Kondo effect with unitary conductance below the Kondo temperature  $T_K = \Lambda_0 \exp[-1/(2J)]$  (Ref. 12) (for experiments in quantum dots see, e.g., Refs. 13). However, for voltages  $V \gg T_K$ , it was argued that the system cannot reach the strong coupling fixed point since the nondiagonal coupling constants,  $J_{LR} = J_{RL}$ , are cut off by the voltage<sup>4,5</sup> and the diagonal ones,  $J_{LL}$  and  $J_{RR}$ , by the voltage-induced decay rate  $\Gamma = \pi J_{LR}^2|_{\Lambda=V} V$ .<sup>5,7</sup> This has raised the fundamental question how decay processes can be implemented in nonequilibrium RG. Applying flow equation methods to the isotropic Kondo model without magnetic field, it was shown within a two-loop formalism in Ref. 7 that the inclusion of a third-order term  $\sim J^3$  in the RG equation leads to a cutoff of the RG flow at the scale  $\Gamma$ .

In this paper, we will analyze this problem from a more general point of view and will show within a microscopic one-loop RG formalism that relaxation and de-

phasing rates will always cut off the RG flow for an arbitrary quantum dot in the Coulomb blockade regime. This confirms the conjecture of Refs. 5 and 10 and generalizes the analysis of Ref. 7 to an arbitrary QD (including orbital and spin fluctuations, many levels, interference effects, etc.). We propose to use the real-time RG (RTRG) formalism of Ref. 1 with a cutoff defined in frequency space since this approach directly discusses the time evolution of the reduced density matrix of the dot via a kinetic equation. Within this formalism, the decay rates occur naturally as the negative imaginary parts of the eigenvalues of the kernel determining the dissipative part of the kinetic equation. This has already been demonstrated previously by applying RTRG to the calculation of steady-state transport through quantum dots in the charge fluctuation regime<sup>2</sup> and to the study of the real-time evolution of the occupation probabilities within the spin boson model.<sup>3</sup> Another advantage of the RTRG approach is the fact that the kernel can easily be inserted self-consistently into the one-loop RG equations of the coupling parameters (analogous to self-energy insertions within Green's function techniques), providing the unique possibility to obtain the physical decay rates within a nonequilibrium one-loop RG formalism. In addition, we also provide a microscopic formalism from which all other standard cutoff scales, such as temperature, energy excitations (e.g., magnetic fields), frequencies, and voltages, can be deduced analytically.

The original RTRG<sup>1</sup> was formulated with a cutoff defined in time space for the reservoir correlation function. This makes it technically difficult to apply the formalism to problems where the interaction between dot and reservoirs is nonlinear as it is the case for quantum dots in the cotunneling regime, where orbital and spin fluctuations dominate transport. Therefore, we use in this work a cutoff defined in frequency space but adapt the same formalism to set up the RG equations as in Ref. 1. This

leads to a combined time-frequency formalism since the time-ordering of the renormalized vertices is needed due to their operator nature (the degrees of freedom of the dot are not integrated out within RTRG, and therefore all coupling vertices are operators acting on the dot degree of freedom). The only disadvantage of the analytic formalism presented in this work is still the fact that the irrelevant prefactors of the various decay rates cutting off the RG flow cannot be determined unambiguously; this has to be left for future developments.

First, we apply the formalism to quantum transport through single molecular magnets (SMM). Recently, it has been shown that the study of Kondo physics can be used for transport spectroscopy of SMM,<sup>14,15</sup> i.e., the various anisotropy parameters determining the spin excitation spectrum can be identified. In the regime where the Kondo temperature is smaller than the distance to the next spin excitation, it has been shown that a pseudo-spin-1/2 model can be derived which can be mapped onto the fully anisotropic Kondo model with three different exchange couplings  $J_x$ ,  $J_y$ , and  $J_z$ . Interestingly, this model reveals a quantum phase transition by changing the sign of  $J_x J_y J_z$ , separating the flow to the weak and strong coupling regimes. Since the exchange couplings depend on the transverse anisotropy parameters, which in turn depend on the coupling of the SMM to the leads, this phase transition can be tuned in an experimental setup. Using RTRG, we calculate the differential conductance  $G(V)$  as function of bias voltage at finite magnetic field and show that the Kondo-enhanced conductance at  $V = h$ , where  $h$  is the level spacing between the ground state and the first excited state, disappears by tuning the system through the phase transition.

Second, we calculate the quantum noise  $S(\Omega)$  as function of frequency for the isotropic Kondo model at finite bias and zero magnetic field. We find that the dephasing rate can be identified by studying the derivative of the noise near  $\Omega = V$ . Specifically, it turns out that the noise has a dip at  $V = \Omega$  (see also Ref. 16, where the noise has been calculated for the Toulouse point), whereas the derivative  $dS(\Omega)/d\Omega$  shows a characteristic shoulder with a height depending on the dephasing rate.

The paper is organized as follows: In Sec. II, we set up the general model and show the relation to the nonequilibrium Kondo model. Section III summarizes the diagrammatic language in Liouville space. Section IV is the central technical part where we set up the RG equations and explain how decay rates cut off the RG flow. Finally, we apply the formalism in Sec. V to transport through single molecular magnets and in Sec. VI to the calculation of quantum noise. Two appendices provide further details of the RG formalism.

## II. MODEL

We consider an arbitrary quantum dot coupled to reservoirs via tunneling processes,

$$H = H_{\text{res}} + H_{\text{D}} + H_{\text{T}}, \quad (1)$$

where  $H_{\text{res}}$ ,  $H_{\text{D}}$ , and  $H_{\text{T}}$  denote the Hamiltonians of the reservoirs, the dot, and the tunneling, respectively.

$$H_{\text{res}} = \sum_{\alpha} H_{\text{res}}^{\alpha} = \sum_{k\alpha\sigma} \epsilon_{k\alpha\sigma} a_{k\alpha\sigma}^{\dagger} a_{k\alpha\sigma} \quad (2)$$

describes the noninteracting Hamiltonian of the reservoirs with  $a_{k\alpha\sigma}^{\dagger}$  ( $a_{k\alpha\sigma}$ ) the creation (annihilation) operators.  $\alpha$  is the reservoir index,  $\sigma$  denotes the spin, and  $k$  is an index for the single-particle states in the reservoirs. Each reservoir is assumed to be infinitely large and described by a grand canonical distribution with electrochemical potential  $\mu_{\alpha}$  and temperature  $T$ . The isolated dot Hamiltonian is written in diagonalized form as

$$H_{\text{D}} = \sum_s E_s |s\rangle\langle s|, \quad (3)$$

where  $s$  is an index for the many-body eigenstates of the dot with energy eigenvalues  $E_s$ . Finally, the interaction between dot and reservoirs is described by the standard tunneling Hamiltonian

$$H_{\text{T}} = \sum_{\alpha k l \sigma} t_{kl}^{\alpha\sigma} a_{k\alpha\sigma}^{\dagger} c_{l\sigma} + \text{H.c.}, \quad (4)$$

where  $c_{l\sigma}$  annihilates a particle with spin  $\sigma$  in the single-particle level  $l$  on the dot and  $t_{kl}^{\alpha\sigma}$  denotes the tunneling matrix element.

Since the reservoirs are infinitely large, we describe their spectrum by the continuum density of states  $\rho_{\mu}(\omega) = \sum_k \delta(\omega - \epsilon_{k\mu} + \mu_{\alpha})$ , with  $\mu \equiv \alpha\sigma$  an index containing the reservoir and the spin index (this will be used implicitly in the following). For the general discussion, we include the case of spin- and frequency-dependent density of states in the reservoirs. We introduce the continuum fields

$$a_{\mu+}(\omega) = \frac{1}{\sqrt{\rho_{\mu}(\omega)}} \sum_k \delta(\omega - \epsilon_{k\mu} + \mu_{\alpha}) a_{k\mu}^{\dagger} \quad (5)$$

and  $a_{\mu-}(\omega) = a_{\mu+}(\omega)^{\dagger}$  which fulfill the anticommutation relation  $\{a_{\mu\eta}(\omega), a_{\mu'\eta'}(\omega')\} = \delta_{\eta,-\eta'} \delta_{\mu\mu'} \delta(\omega - \omega')$ . With this notation, the reservoir Hamiltonian and the tunneling part can be written as

$$H_{\text{res}} = \sum_{\mu} \int d\omega (\omega + \mu_{\alpha}) a_{\mu+}(\omega) a_{\mu-}(\omega), \quad (6)$$

$$H_{\text{T}} = \sum_{\mu} \int d\omega a_{\mu+}(\omega) g_{\mu}(\omega) + \text{H.c.}, \quad (7)$$

with

$$g_{\mu}(\omega) = \sqrt{\rho_{\mu}(\omega)} \sum_l t_l^{\mu}(\omega) c_{l\sigma}, \quad (8)$$

where  $t_l^{\alpha\sigma}(\omega) \equiv t_{kl}^{\alpha\sigma}$  is the tunneling matrix element in the continuum notation evaluated for reservoir state  $k$  such that  $\epsilon_{k\alpha\sigma} - \mu_\alpha = \omega$ . The contraction of two reservoir field operators with respect to the equilibrium reservoir distribution is given by

$$\langle a_{\mu\eta}(\omega)a_{\mu'\eta'}(\omega') \rangle_{\text{res}} = \delta_{\eta,-\eta'} \delta_{\mu\mu'} \delta(\omega - \omega') \theta_\omega f_\omega^\eta, \quad (9)$$

where  $f_\omega^+ = f_\omega$  and  $f_\omega^- = 1 - f_\omega = f_{-\omega}$ , with  $f_\omega = 1/[\exp(\beta\omega) + 1]$  denoting the Fermi function (note that the different electrochemical potentials of the reservoirs occur in our notation via the interaction picture from the time-dependence of the field operators).  $\theta_\omega = \theta(\Lambda_0 - \omega)$  contains the initial band width  $\Lambda_0$  of the reservoirs (which are assumed to be all the same relative to the corresponding electrochemical potentials).

We now consider a quantum dot in the Coulomb blockade regime, i.e., the total charge is fixed, and only cotunneling processes via virtual intermediate states can lead to orbital and spin fluctuations. The effective Hamiltonian in this regime is standardly derived using the Schrieffer-Wolff transformation,<sup>17</sup> leading to

$$H_{\text{eff}} = H_{\text{res}} + H_{\text{D}} + V_{\text{eff}}, \quad (10)$$

with

$$V_{\text{eff}} = \sum_{\mu\mu'} \int_{-\Lambda_0}^{\Lambda_0} d\omega d\omega' \left\{ g_{\mu\mu'}^+(\omega, \omega') a_{\mu+}(\omega) a_{\mu'-}(\omega') - g_{\mu\mu'}^-(\omega, \omega') a_{\mu'-}(\omega') a_{\mu+}(\omega) \right\}, \quad (11)$$

where

$$g_{\mu\mu'}^+(\omega, \omega') = \frac{1}{2} \sum_{ss'} |s\rangle \langle s'| \cdot \langle s | g_\mu(\omega) \quad (12)$$

$$\left( \frac{1}{\omega + \mu_\alpha + E_s - H_{\text{D}}} + \frac{1}{\omega' + \mu_{\alpha'} + E_{s'} - H_{\text{D}}} \right) g_{\mu'}(\omega')^\dagger |s'\rangle$$

corresponds to virtual processes, where the electron first hops from the reservoir to the dot and then back, and

$$g_{\mu\mu'}^-(\omega, \omega') = \frac{1}{2} \sum_{ss'} |s\rangle \langle s'| \cdot \langle s | g_{\mu'}(\omega')^\dagger \quad (13)$$

$$\left( \frac{1}{\omega + \mu_\alpha - E_{s'} + H_{\text{D}}} + \frac{1}{\omega' + \mu_{\alpha'} - E_s + H_{\text{D}}} \right) g_\mu(\omega) |s'\rangle$$

describes the reverse process. Processes where two electrons hop on or off the dot are not written here but can easily be incorporated (they are only important for molecular systems with negative Coulomb interaction; see Ref. 18).

In normal-ordered form (with respect to the equilibrium reservoir distribution), denoted by the symbol  $:\dots:$ , we get from Eqs (10), (11), and (9)

$$H_{\text{eff}} = H_{\text{res}} + H_{\text{D}}^{\text{eff}} + :V_{\text{eff}}:, \quad (14)$$

with a renormalized dot Hamiltonian

$$H_{\text{D}}^{\text{eff}} = H_{\text{D}} + \sum_{\mu\eta} \int d\omega \theta_\omega \eta g_{\mu\mu}^\eta(\omega, \omega) f_\omega^\eta, \quad (15)$$

which can contain logarithmic energy renormalizations of the dot states due to orbital interferences or due to spin-dependent tunneling matrix elements (see, e.g., Refs. 19 and 20) (for the Kondo model under consideration in this work, such renormalizations do not occur). Finally, the normal-ordered interaction term reads

$$V \equiv: V_{\text{eff}}: = \sum_{\mu\mu'} \int_{-\Lambda_0}^{\Lambda_0} d\omega d\omega' g_{\mu\mu'}(\omega, \omega') : a_{\mu+}(\omega) a_{\mu'-}(\omega') :, \quad (16)$$

with

$$g_{\mu\mu'}(\omega, \omega') = \sum_{\eta} g_{\mu\mu'}^\eta(\omega, \omega'). \quad (17)$$

Equations (14) and (16) are the final general form of the model under consideration, which is the starting point for the renormalization group formalism. It is still completely general, except for the fact that the dot is assumed to be at fixed charge. In order to simplify the notation, we omit in the following the index ‘‘eff’’, and use the short-hand notation

$$V = g_{11'} : a_{1+} a_{1'-} :, \quad (18)$$

where we sum/integrate implicitly over the indices  $1 \equiv \omega_1 \mu_1$  and  $1' \equiv \omega_{1'} \mu_{1'}$ . We note the property

$$g_{11'} = g_{1'1}^*, \quad (19)$$

which guarantees the Hermiticity of  $H_{\text{D}}$ .

The fully anisotropic Kondo model under consideration in Sec. V is realized for the special case where the dot Hamiltonian consists of two states with (pseudo-) spin up or down (i.e.,  $s = \pm = \uparrow, \downarrow$  denotes the dot spin). The antiferromagnetic exchange processes between the dot spin  $\underline{s}$  and the reservoir spins are described by the coupling

$$g_{11'} = \frac{1}{2} \sum_{i=x,y,z} J_{\alpha_1 \alpha'_1}^i S^i \sigma_{\sigma_1 \sigma'_1}^i, \quad (20)$$

where  $\sigma^i$ ,  $i = x, y, z$ , are the Pauli matrices. Inserting this into Eq. (16) gives the standard form of the anisotropic Kondo model,

$$H_{\text{D}} = \frac{h}{2} \sum_{s=\pm} s |s\rangle \langle s|, \quad (21)$$

$$V = \frac{1}{2} \sum_{i\mu\mu'} \int_{-\Lambda_0}^{\Lambda_0} d\omega d\omega' J_{\alpha\alpha'}^i S^i \sigma_{\sigma\sigma'}^i : a_{\mu+}(\omega) a_{\mu'-}(\omega') :, \quad (22)$$

where  $h$  denotes the effective magnetic field in the  $z$  direction. In contrast to the usual case  $J^x = J^y$ , we discuss here the fully anisotropic Kondo model with three different exchange couplings, a model of recent interest if

the dot is replaced by a single molecular magnet.<sup>14</sup> In this case, the isolated molecule is described by the spin Hamiltonian

$$H_{\text{mol}} = -D(S_M^z)^2 - \frac{1}{2} \sum_n B_{2n} [(S_M^+)^{2n} + (S_M^-)^{2n}] + h_z S_M^z, \quad (23)$$

where  $D$  and  $B_{2n}$  denote the longitudinal and transverse anisotropy constants, and the original spin  $S_M$  is greater than  $1/2$ .  $h_z$  denotes the physical magnetic field in the  $z$  direction. If one projects an isotropic exchange  $(J/2)\underline{S}_M \underline{\sigma}_{\sigma\sigma'} a_{\mu+}(\omega) a_{\mu'-}(\omega')$  between the molecule and reservoirs onto the two lowest eigenstates  $|\pm\rangle$  of  $H_{\text{mol}}$  (which is justified when the Kondo temperature is lower than the first magnetic excitation), one obtains a pseudo-spin-1/2 model described by the fully anisotropic Kondo model [Eqs. (21) and (22)] with

$$h = \langle +|H_{\text{mol}}|+ \rangle - \langle -|H_{\text{mol}}|- \rangle, \quad (24)$$

$$J^{x/y} = J \langle +|S_M^{\pm} \pm S_M^{\mp}|- \rangle, \quad (25)$$

$$J^z = 2J \langle +|S_M^z|+ \rangle > 0, \quad (26)$$

where  $J$  is the isotropic exchange constant between the original molecular spin and the reservoirs (see Ref. 14 for further details).

### III. PERTURBATION SERIES

We aim at calculating the stationary dot distribution  $p^{\text{st}}$ , the stationary current  $I_{\text{st}}^{\gamma}$  in lead  $\gamma$ , and the frequency-dependent noise power

$$\begin{aligned} S_{\Omega}^{\gamma\gamma'} &= \frac{1}{2} \int dt e^{i\Omega t} \langle \{ \delta I^{\gamma}(t), \delta I^{\gamma'}(0) \} \rangle \\ &= \bar{S}_{-\Omega}^{\gamma\gamma'} + \bar{S}_{\Omega}^{\gamma'\gamma} - 2\pi \delta(\Omega) I_{\text{st}}^{\gamma} I_{\text{st}}^{\gamma'}, \end{aligned} \quad (27)$$

with  $\delta I^{\gamma} = I^{\gamma} - I_{\text{st}}^{\gamma}$  and

$$\bar{S}_{\Omega}^{\gamma\gamma'} = \frac{1}{2} \int_{-\infty}^0 dt e^{-i\Omega t} \langle \{ I^{\gamma}(t), I^{\gamma'}(0) \} \rangle. \quad (28)$$

Due to current conservation, we have

$$\sum_{\gamma} S_{\Omega}^{\gamma\gamma'} = \sum_{\gamma'} S_{\Omega}^{\gamma\gamma'} = 0, \quad (29)$$

and therefore, for two reservoirs, it is sufficient to calculate the diagonal noise  $S^{\gamma\gamma}$ .

The current operator  $I^{\gamma}$  for lead  $\gamma$  is given by  $I^{\gamma} = -(d/dt)N_{\gamma} = -i[V, N_{\gamma}]$ , where  $N_{\gamma}$  is the particle number in reservoir  $\gamma$  (we use units  $e = \hbar = 1$ ). Using Eq. (18), this gives

$$I^{\gamma} = i(\delta_{\gamma\alpha_1} - \delta_{\gamma\alpha'_1}) g_{11'} : a_{1+} a_{1'-} : . \quad (30)$$

Following Ref. 1, we start from an initial distribution  $\rho(t_0) = p(t_0)\rho_{\text{res}}$  which factorizes into an arbitrary dot

part  $p(t_0)$  and an equilibrium grand canonical distribution  $\rho_{\text{res}} = \Pi_{\alpha} \exp[-\beta(H_{\text{res}}^{\alpha} - \mu_{\alpha} N_{\alpha})]/Z_{\alpha}$  for the reservoirs. The reduced density matrix of the dot at time  $t$  can then be written as

$$p(t) = \text{Tr}_{\text{res}} e^{-iL(t-t_0)} p(t_0) \rho_{\text{res}}, \quad (31)$$

where  $L = [H, \cdot]$  is the Liouville operator, which is a superoperator acting on ordinary operators  $b$  via  $Lb = [H, b]$ . According to Eq. (14), we decompose  $L = L_{\text{res}} + L_{\text{D}} + L_{\text{V}}$ . Using Eq. (18), the Liouville operator of the interaction part can be written as

$$L_{\text{V}} = [V, \cdot] = p' G_{11'}^{pp'} : J_{1+}^p J_{1'-}^{p'} :, \quad (32)$$

where we sum implicitly over the Keldysh indices  $p, p' = \pm$ . Here,

$$G_{11'}^{pp'} = \delta_{pp'} G_{11'}^{pp}, \quad (33)$$

and  $J_{1\eta}^p$  are superoperators acting on usual dot (lead) operators  $b$  via

$$G_{11'}^{++} b = g_{11'} b, \quad G_{11'}^{--} b = -b g_{11'}, \quad (34)$$

$$J_{1\eta}^{+} b = a_{1\eta} b, \quad J_{1\eta}^{-} b = b a_{1\eta}. \quad (35)$$

Taking matrix elements with respect to the dot states, the superoperators  $L_{\text{D}}$  and  $G_{11'}^{pp}$  are given by

$$(L_{\text{D}})_{s_1 s'_1, s_2 s'_2} = (H_{\text{D}})_{s_1 s_2} \delta_{s'_1 s'_2} - \delta_{s_1 s_2} (H_{\text{D}})_{s'_2 s'_1}, \quad (36)$$

$$(G_{11'}^{++})_{s_1 s'_1, s_2 s'_2} = (g_{11'})_{s_1 s_2} \delta_{s'_1 s'_2}, \quad (37)$$

$$(G_{11'}^{--})_{s_1 s'_1, s_2 s'_2} = -\delta_{s_1 s_2} (g_{11'})_{s'_2 s'_1}. \quad (38)$$

If the states  $|s\rangle$  are the eigenstates of  $H_{\text{D}}$  with eigenvalues  $E_s$ , we get

$$(L_{\text{D}})_{s_1 s'_1, s_2 s'_2} = (E_{s_1} - E_{s'_1}) \delta_{s_1 s_2} \delta_{s'_1 s'_2}. \quad (39)$$

From these matrix representations, we get

$$\sum_s (L_{\text{D}})_{ss, \dots} = 0, \quad \sum_p \sum_s (G_{11'}^{pp})_{ss, \dots} = 0, \quad (40)$$

which is an important property guaranteeing the conservation of probability  $\sum_s p(t)_{ss} = 1$  (see Ref. 1).

Following Ref. 1, we expand Eq. (31) in  $L_{\text{V}}$  and integrate out the leads in order to get an effective description for the dynamics of the dot. We define the interaction picture of  $L_{\text{V}}$  with respect to  $L_{\text{res}} + L_{\text{D}}$  and obtain  $L_{\text{V}}(t) = p' G_{11', t}^{pp'} : J_{1+}^p J_{1'-}^{p'} :,$  with

$$G_{11', t}^{pp'} = e^{i(\omega_1 - \omega'_1 + \mu_{\alpha_1} - \mu_{\alpha'_1})t} e^{iL_{\text{D}} t} G_{11'}^{pp'} e^{-iL_{\text{D}} t}. \quad (41)$$

Each term in the perturbation expansion is then averaged over the equilibrium reservoir distribution by using Wick's theorem. Using Eq. (9), this leads to pair contractions between the superoperators  $J_{1\eta}^p$  given by

$$\gamma_{1\eta, 1'\eta'}^{pp'} = \overline{J_{1\eta}^p J_{1'\eta'}^{p'}} = \langle J_{1\eta}^p J_{1'\eta'}^{p'} \rangle = \delta_{11'} \delta_{\eta, -\eta'} f_{\omega_1}^{p'} \theta_{\omega_1}. \quad (42)$$

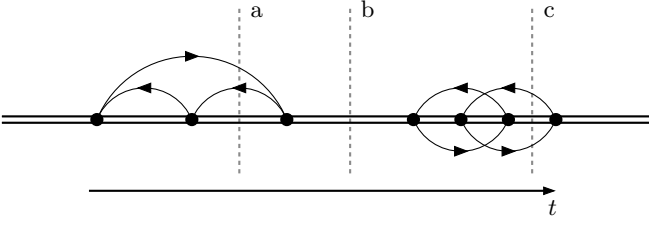


FIG. 1: Example of a sequence of two irreducible blocks. The double line represents time propagation in Liouville space of the dot (time increases to the right). The black dots represent the vertices  $G_{11'}^{pp'}$ . The lines connecting the vertices are the reservoir contractions. Whereas the auxiliary vertical lines  $a$  and  $c$  hit reservoir contractions, line  $b$  does not and separates the two irreducible blocks.

In this way, we obtain a sequence of time-ordered dot superoperators  $(-i)G_{11',t}^{pp'}$  in interaction picture, connected in an arbitrary way by lead contractions (for details and diagrammatic representations on the time axis, see Ref. 1).

The series of all diagrams can be grouped in irreducible and reducible parts, where irreducible means that any vertical cut to the time axis hits at least one reservoir contraction (see Fig. 1 for an example). We define the kernel  $\Sigma_\Omega = \int_0^\infty dt e^{i\Omega t} \Sigma(t)$  in Laplace space, where  $\Sigma(t)$  is the sum of all irreducible diagrams between time 0 and  $t$ . The whole series of all diagrams can then be formally resummed and we obtain the following result for the dot distribution in Laplace space:

$$p_\Omega = \Pi_\Omega p(t_0), \quad \Pi_\Omega = \frac{i}{\Omega - L_D - i\Sigma_\Omega}, \quad (43)$$

with  $p_\Omega = \int_{t_0}^\infty dt e^{i\Omega t} p(t)$ . The stationary distribution follows from  $p^{\text{st}} = -i \lim_{\Omega \rightarrow 0} \Omega p_\Omega$ , leading to

$$(L_D + i\Sigma) p^{\text{st}} = 0, \quad (44)$$

where  $\Sigma = \Sigma_{\Omega=0}$ . Therefore, the central quantity to be calculated within renormalization group is the irreducible kernel  $\Sigma$ ; the stationary distribution then follows from finding the eigenvector with eigenvalue zero of  $L_D + i\Sigma$ . We note that the irreducible kernel starts and ends with two boundary vertices, denoted by  $B$  and  $A$ , respectively. Compared to Eq. (41), their interaction picture is slightly differently defined and contains the frequency  $\Omega$ ,

$$A_{11',\Omega,t}^{pp'} = e^{i\Omega t} e^{i(\omega_1 - \omega'_1 + \mu_{\alpha_1} - \mu_{\alpha'_1})t} A_{11',\Omega}^{pp'} e^{-iL_D t}, \quad (45)$$

$$B_{11',\Omega,t}^{pp'} = e^{-i\Omega t} e^{i(\omega_1 - \omega'_1 + \mu_{\alpha_1} - \mu_{\alpha'_1})t} e^{iL_D t} B_{11',\Omega}^{pp'}. \quad (46)$$

Before starting the RG, we have  $A_{11',\Omega}^{pp'} = B_{11',\Omega}^{pp'} = G_{11'}^{pp'}$ , but during RG, the boundary vertices renormalize differently and can become  $\Omega$  dependent.

A similar approach can be set up for the calculation of current and noise. Choosing  $t_0 = 0$ , we write for the

current in Laplace space

$$I_\Omega^\gamma = \int_0^\infty e^{i\Omega t} \text{Tr} T[-iL_V^\gamma(t)] e^{-i \int_0^t dt' L_V(t')} p(0) \rho_{\text{res}}, \quad (47)$$

where  $T$  is the time-ordering symbol and

$$L_V^\gamma = \frac{1}{2} i \{I^\gamma, \cdot\} = p' G_{11'}^{\gamma, pp'} : J_{1+}^p J_{1-}^{p'} : \quad (48)$$

is the current superoperator. The current vertex in Liouville space is given by

$$G_{11'}^{\gamma, pp'} = c_{\alpha_1 \alpha'_1}^\gamma p' G_{11'}^{pp'}, \quad (49)$$

with

$$c_{\alpha\alpha'}^\gamma = -\frac{1}{2} (\delta_{\gamma\alpha} - \delta_{\gamma\alpha'}). \quad (50)$$

Expanding the exponential as described above in  $L_V$ , integrating out the reservoirs, and resumming the whole series using the irreducible blocks, one arrives at

$$I_\Omega^\gamma = \text{Tr}_D \Sigma_\Omega^\gamma p_\Omega, \quad (51)$$

and the stationary current follows from

$$I_{\text{st}}^\gamma = \text{Tr}_D \Sigma^\gamma p^{\text{st}}, \quad (52)$$

with  $\Sigma^\gamma = \Sigma_{\Omega=0}^\gamma$ . Here,  $\text{Tr}_D$  denotes the trace over the dot states and  $\Sigma_\Omega^\gamma$  is the irreducible kernel containing exactly one current vertex  $G_{11'}^{\gamma, pp'}$  with interaction picture defined by

$$G_{11',\Omega,t}^{\gamma, pp'} = e^{i\Omega t} e^{i(\omega_1 - \omega'_1 + \mu_{\alpha_1} - \mu_{\alpha'_1})t} e^{iL_D t} G_{11',\Omega}^{\gamma, pp'} e^{-iL_D t}. \quad (53)$$

For the noise, we choose  $t_0 = -\infty$  and start from the expression

$$\begin{aligned} \bar{S}_\Omega^{\gamma\gamma'} &= \int_{-\infty}^0 dt e^{-i\Omega t} \text{Tr} T[-iL_V^\gamma(0)][-iL_V^{\gamma'}(t)] \\ &\quad \times e^{-i \int_{-\infty}^0 dt' L_V(t')} p(-\infty) \rho_{\text{res}}. \end{aligned} \quad (54)$$

Again, expanding in  $L_V$ , integrating out the reservoirs, and resumming via irreducible blocks gives

$$\bar{S}_\Omega^{\gamma\gamma'} = \text{Tr}_D (\Sigma_\Omega^{\gamma\gamma'} + \Sigma_\Omega^\gamma \Pi_\Omega \Sigma_\Omega^{\gamma'\dagger}) p^{\text{st}}, \quad (55)$$

with  $\Sigma_\Omega^{\gamma\gamma'}$  the irreducible kernel containing exactly two current vertices (see also Ref. 21). Since the current vertices can also lie at the two boundaries of the kernel, one has to define several boundary current vertices with slightly different interaction picture compared to Eq. (53) (see Appendix B for more details).

#### IV. RENORMALIZATION GROUP FORMALISM AND CUTOFF SCALES

We now take a reduced band width  $\Lambda$  in the definition of the contraction [Eq. (42)] by replacing  $\theta_\omega \rightarrow \theta(\Lambda - |\omega|)$ . Following Ref. 1, we determine the  $\Lambda$ -dependence of  $L_D$  and  $G_{11'}$  in such a way that the total sum of all diagrams remains invariant. This leads to the RG diagrams of Fig. 2 which are evaluated in Appendix A with the result

$$\left(\frac{dG_{11'}^{p_1 p_1'}}{d\Lambda}\right)_{ik} = i \int_0^{\Gamma_j^{-1}} dt \delta_{\omega_2} \times \left\{ p_2' f_{\omega_2}^{-p_2'} (G_{12,t/2}^{p_1 p_2})_{ij} (G_{21',-t/2}^{p_2' p_1'})_{jk} - p_2 f_{\omega_2}^{p_2} (G_{21',t/2}^{p_2 p_1'})_{ij} (G_{12,-t/2}^{p_1 p_2})_{jk} \right\}, \quad (56)$$

$$\left(\frac{dL_D}{d\Lambda}\right)_{ik} = i \int_0^{\Gamma_j^{-1}} dt \frac{d}{d\Lambda} (\theta_{\omega_1} \theta_{\omega_2}) p_2 p_2' f_{\omega_1}^{p_2} f_{\omega_2}^{-p_2} (G_{12,t/2}^{p_1 p_1'})_{ij} (G_{21,-t/2}^{p_2 p_2'})_{jk}, \quad (57)$$

with  $\delta_\omega = \delta(\Lambda - |\omega|)$ .  $(G)_{ij} = \langle i|G|j \rangle$  denotes the matrix element with respect to the eigenvectors of  $L_D$ ,

$$L_D |j\rangle = \lambda_j |j\rangle, \quad \lambda_j = h_j - i\Gamma_j. \quad (58)$$

$h$  and  $\Gamma > 0$  describe dot excitations and decay rates, respectively. Since  $\Gamma$  leads to exponential damping between the vertices, the time integrals can be cut off by  $\Gamma^{-1}$ , thereby neglecting only small perturbative corrections for energy scales below  $\Gamma$ . Note, however, that  $L_D$  has a unique eigenvector  $|0\rangle$  with zero eigenvalue since the system is approaching a stationary state.<sup>22</sup> Therefore, the contribution from this eigenvector does not lead to exponential damping but it will be shown below that it does not contribute to the RG flow in leading order. For later purpose, we note that the ‘‘ket’’ form  $\langle ss'|0\rangle$  depends on the specific problem under consideration, but the ‘‘bra’’ form  $\langle 0|ss'\rangle$  is unique and is given by

$$\langle 0|ss'\rangle = \frac{1}{\sqrt{Z}} \delta_{ss'}, \quad (59)$$

where  $Z$  is the number of many-particle states considered on the dot. This property follows directly from Eq. (40).

Using Eqs. (41) and (58), we obtain the following expression for the time integral in Eq. (56) [ $\pm$  corresponds to the two terms on the right hand side (rhs)]:

$$i \int_0^{\Gamma_j^{-1}} dt e^{\mp i(\omega_2 + x_\pm)t} e^{-(\Gamma_j - \Gamma_{ik})t} = \frac{1 - e^{\mp i(\omega_2 + x_\pm \mp i(\Gamma_j - \Gamma_{ik}))/\Gamma_j}}{\pm(\omega_2 + x_\pm) - i(\Gamma_j - \Gamma_{ik})}, \quad (60)$$

with  $|\omega_2| = \Lambda$ ,  $\lambda_{ik} = (\lambda_i + \lambda_k)/2 = h_{ik} - i\Gamma_{ik}$ ,  $x_\pm = \mu_{\alpha_2} - \mu_{\alpha_1 \alpha_1'} - \omega_{11'} \pm (h_j - h_{ik})$ ,  $\mu_{\alpha_1 \alpha_1'} = (\mu_{\alpha_1} + \mu_{\alpha_1'})/2$ , and  $\omega_{11'} = (\omega_1 + \omega_1')/2$ . This provides a cutoff at

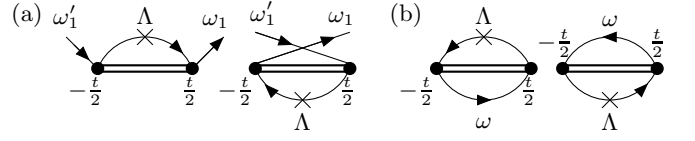


FIG. 2: The RG diagrams determining the renormalization of (a)  $G$  and (b)  $L_D$ . The cross indicates differentiation of the lead contractions with respect to  $\Lambda$ . Time-ordering is defined with respect to the middle time.

$\Lambda_\pm = \max(|x_\pm|, \Gamma_j, |\Gamma_j - \Gamma_{ik}|)$ , containing frequencies, voltages, dot excitation energies, and decay rates. Above the cutoffs, we obtain  $\pm \text{sign}(\omega_2)/\Lambda$  for Eq. (60). Therefore, we can replace  $-\text{sign}(\omega_2) p f^p(\omega_2)$  by  $\text{sign}(\omega_2) p [1/2 - f^p(\omega_2)] = 1/2 - f(\Lambda) \approx (1/2)\theta_T$  in Eq. (56), providing the cutoff set by temperature. This gives

$$(dG_{11'}^{p_1 p_1'}/dl)_{ik} = -\frac{1}{2} \theta_T \delta_{\omega_2} \times \left\{ \theta_{\Lambda_+} (G_{12}^{p_1 p_2})_{ij} (G_{21'}^{p_2' p_1'})_{jk} - \theta_{\Lambda_-} (G_{21'}^{p_2' p_1'})_{ij} (G_{12}^{p_1 p_2})_{jk} \right\}, \quad (61)$$

where  $l = \ln(\Lambda_0/\Lambda)$  denotes the flow parameter. First, we get from this equation the central result that decay rates always lead to a cutoff of the RG flow. If all  $i, j, k$  correspond to the eigenvector with zero eigenvalue, we get  $\Lambda_+ = \Lambda_-$  and the two terms on the rhs of Eq. (61) cancel. If at least one eigenvector has nonzero eigenvalue, we obtain a cutoff either from  $\Gamma_j$  or  $|\Gamma_j - \Gamma_{ik}|$ . Neglecting the irrelevant difference between the various decay rates, we replace them in the following by an overall scale  $\Gamma$ . Second, above all cutoff scales, the RG equation preserves the initial form of the vertex given by Eqs. (33) and (34). Below, we show that a similiar analysis leads to  $L_D = [H_D, \cdot]$  in leading order, with  $H_D = \sum_s E_s |s\rangle \langle s|$  denoting the renormalized dot Hamiltonian [see Eq. (66)]. Inserting these forms in Eq. (61), we can project the RG equation for the vertex on one part of the Keldysh contour and we obtain the final result

$$(dg_{11'}/dl)_{ss'} = -\frac{1}{2} \delta_{\omega_2} \times \left\{ \theta_{\max(T, |x_+|, \Gamma)} (g_{12})_{s\bar{s}} (g_{21'})_{\bar{s}s'} - \theta_{\max(T, |x_-|, \Gamma)} (g_{21'})_{s\bar{s}} (g_{12})_{\bar{s}s'} \right\}, \quad (62)$$

with  $x_\pm = \mu_{\alpha_2} - \mu_{\alpha_1 \alpha_1'} - \omega_{11'} \pm (E_{\bar{s}} - E_{ss'})$  and  $E_{ss'} = (E_s + E_{s'})/2$ . If the frequency dependence is irrelevant, we get  $g_{\mu\mu'}(\omega_1, \omega_1') = g_{\mu\mu'}(\omega_{11'})$ . This equation is a generalization of the RG equation of Ref. 5 to an arbitrary QD in the CB regime with (possibly) frequency dependent density of states in the leads, including the microscopically derived cutoff scales from decay processes.

We now turn to the leading order analysis for the RG equation (57) of the dot Liouvillian. We first insert the

leading order form (33) for the vertex and get

$$\left(\frac{dL_D}{d\Lambda}\right)_{ik} = i \int_0^{\Gamma_j^{-1}} dt \frac{d}{d\Lambda} (\theta_{\omega_1} \theta_{\omega_2}) f_{\omega_1}^{p'} f_{\omega_2}^{-p'} (G_{12,t/2}^{pp})_{ij} (G_{21,-t/2}^{p'p'})_{jk}. \quad (63)$$

Using  $(d/d\Lambda)\theta_{\omega_1}\theta_{\omega_2} = \theta_{\omega_1}\delta_{\omega_2} + \delta_{\omega_1}\theta_{\omega_2}$  and interchanging  $1 \leftrightarrow 2$  in the second term, we get

$$\begin{aligned} \left(\frac{dL_D}{d\Lambda}\right)_{ik} &= i \int_0^{\Gamma_j^{-1}} dt \delta_{\omega_2} \theta_{\omega_1} \\ &\times \left\{ f_{\omega_1}^{p'} f_{\omega_2}^{-p'} (G_{12,t/2}^{pp})_{ij} (G_{21,-t/2}^{p'p'})_{jk} + \right. \\ &\left. + f_{\omega_1}^{-p} f_{\omega_2}^p (G_{21,t/2}^{p'p'})_{ij} (G_{12,-t/2}^{pp})_{jk} \right\}. \quad (64) \end{aligned}$$

Performing the same steps as for the derivation of Eq. (61), we obtain in leading order

$$\begin{aligned} \left(\frac{dL_D}{d\Lambda}\right)_{ik} &= \frac{1}{2\Lambda} \theta_T \delta_{\omega_2} \theta_{\omega_1} \\ &\times \left\{ \theta_{\Lambda_+} p' f_{\omega_1}^{p'} (G_{12}^{pp})_{ij} (G_{21}^{p'p'})_{jk} + \right. \\ &\left. + \theta_{\Lambda_-} p f_{\omega_1}^{-p} (G_{21}^{p'p'})_{ij} (G_{12}^{pp})_{jk} \right\}, \quad (65) \end{aligned}$$

with  $\Lambda_{\pm} = \max(|x_{\pm}|, \Gamma_j, |\Gamma_j - \Gamma_{ik}|)$  and  $x_{\pm} = \mu_{\alpha_2} - \mu_{\alpha_1} - \omega_1 \pm (h_j - h_{ik})$ . Analogous to the conclusion drawn from Eq. (61), we see that decay rates will always lead to a cutoff of the RG flow for  $L_D$ . Here, the case that  $i \equiv 0$  corresponds to the eigenvector with eigenvalue zero can be excluded, since  $\sum_p \langle 0 | G_{12}^{pp} = 0$  due to Eq. (59) and the property (40) which is conserved under the RG flow. Second, due to the leading order form (34) of the vertex,  $G_{12}^{++} = g_{12}$  acts only on the upper part of the Keldysh contour and  $G_{12}^{--} = -g_{12}$  only on the lower one. Therefore, they commute, and above all cutoff scales (i.e., for  $\Lambda \gg \Lambda_{\pm}$ ), we obtain no contribution from  $p' = -p$  to the renormalization of  $L_D$ . The contribution from  $p' = p$  gives the leading order form  $L_D^{\text{rel}} = [H_D, \cdot]$  with a Hermitian renormalized dot Hamiltonian  $H_D$ . In analogy to Eq. (62), the RG equation for  $H_D$  reads

$$\begin{aligned} (dH_D/d\Lambda)_{ss'} &= \frac{1}{2\Lambda} \delta_{\omega_2} \theta_{\omega_1} \\ &\times \left\{ \theta_{\max(T, |x_+|, \Gamma)} f_{\omega_1}^+ (g_{12})_{s\bar{s}} (g_{21})_{\bar{s}s'} \right. \\ &\left. + \theta_{\max(T, |x_-|, \Gamma)} f_{\omega_1}^- (g_{21})_{s\bar{s}} (g_{12})_{\bar{s}s'} \right\}, \quad (66) \end{aligned}$$

with  $x_{\pm} = \mu_{\alpha_2} - \mu_{\alpha_1} - \omega_1 \pm (E_{\bar{s}} - E_{s'})$ . If the frequency dependence of  $g_{12}$  is irrelevant, we obtain in leading order

$$(dH_D/d\Lambda)_{ss'} = 2\theta_{\max(T, |y|, \Gamma)} (g_{\mu\mu'})_{s\bar{s}} (g_{\mu'\mu})_{\bar{s}s'}, \quad (67)$$

with  $y = \mu_{\alpha} - \mu_{\alpha'} - E_{\bar{s}} + E_{s'}$ .

The RG equations (62) and (66) are the central results of this section. They provide the leading-order renormalization of the vertex and the dot Hamiltonian for a generic quantum dot in the Coulomb blockade regime.

Besides the full frequency dependence and the influence of temperature and voltage, they include the influence of the renormalized dot energies and the decay rates on the RG of the vertex. The renormalized dot energies follow from Eq. (66) but we still have to set up the RG equation for the decay rates  $\Gamma_i$ . They follow from Eq. (63), where we insert on the rhs the leading order form (33) and (34) for the vertex, and the leading order form  $L_D^{\text{rel}} = [H_D, \cdot]$  for the dot Liouvillian, i.e., we neglect essentially the influence of the decay rates on themselves. As shown above, the leading order form  $L_D^{\text{rel}} = [H_D, \cdot]$  arises from the principal value part of the time integral and taking  $p = p'$ . There are two additional contributions to  $L_D$ . The first one arises from  $p = p'$  but taking the  $\delta$ -function part of the time integral. This leads to a contribution of the form  $L_D^{\text{br}} = \{H_D^{\text{br}}, \cdot\}$  with an anti-Hermitian dot Hamiltonian  $H_D^{\text{br}}$  describing energy broadening. The second one arises from  $p = -p'$ , i.e., from diagrams connecting the upper with the lower part of the Keldysh contour. This part is denoted by  $L_D^{\text{rd}}$  and describes the physics of relaxation and dephasing. For  $p = -p'$ , only the  $\delta$ -function part of the time integral contributes and a straightforward calculation gives the results

$$\begin{aligned} -i \left(\frac{dL_D^{\text{rd}}}{d\Lambda}\right)_{s_1 s'_1, s_2 s'_2} &= -2\pi g_{\mu\mu'}(\omega, \omega')_{s_1 s_2} g_{\mu\mu'}(\omega, \omega')_{s'_1 s'_2}^* \\ &\times \frac{d}{d\Lambda} (\theta_{\omega} \theta_{\omega'}) f_{\omega}^- f_{\omega'}^+ \delta(\omega - \omega' + y) \quad (68) \end{aligned}$$

together with

$$(H_D^{\text{br}})_{ss'} = (-1/2) \sum_{\bar{s}} (L_D^{\text{rd}})_{\bar{s}\bar{s}, s's}, \quad (69)$$

where  $y = \mu_{\alpha} - \mu_{\alpha'} + E_1 - E_2$  and  $E_i = E_{s_i s'_i}$ . The frequency integrals over  $\omega$  and  $\omega'$  can be calculated analytically due to the two  $\delta$ -functions. If we take the frequency dependence of the vertex in leading order  $g_{\mu\mu'}(\omega, \omega') = g_{\mu\mu'}(\frac{\omega+\omega'}{2})$ , we obtain explicitly

$$\begin{aligned} -i \left(\frac{dL_D^{\text{rd}}}{d\Lambda}\right)_{s_1 s'_1, s_2 s'_2} &= -2\pi \theta_{|y|/2} \sum_{pp'=\pm} \theta(pp') f_{\Lambda}^p f_{\Lambda}^{-p} \\ &\times g_{\mu\mu'}(p'(\Lambda - |y/2|))_{s_1 s_2} g_{\mu\mu'}(p(\Lambda - |y/2|))_{s'_1 s'_2}^*. \quad (70) \end{aligned}$$

Thus, for  $T = 0$ , we see that decay rates are only generated for  $|y/2| < \Lambda < |y|$ , i.e., essentially below all cutoff scales. The reason for this interval is a simple golden rule argument illustrated in Fig. 3 for the case  $s = s_1 = s'_1$ ,  $s' = s_2 = s'_2$  and  $E_s = E_{s'}$ . Finally, we note that including the influence of the decay rates in the rhs of Eq. (68), one obtains essentially a broadening of the  $\delta$ -function by  $\Gamma$ .

A similar analysis can be used to determine  $\Sigma$ ,  $\Sigma^{\gamma}$ , and  $\Sigma^{\gamma\gamma'}$ . However, since several boundary vertices with different cutoff scales have to be distinguished for the general case, we summarize here only those matrix elements necessary for the Kondo model [Eq. (22)] (for

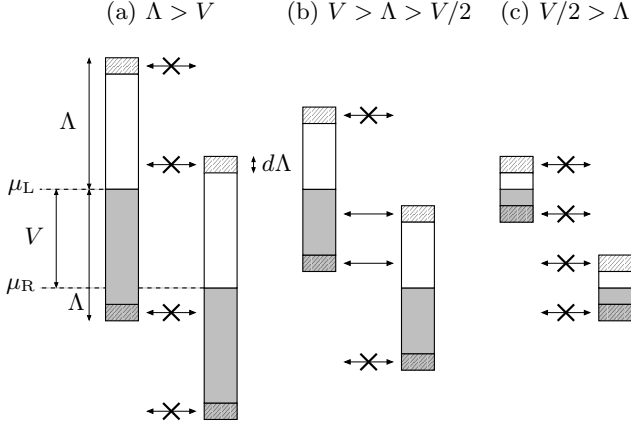


FIG. 3: Generation of a transition rate from state  $s$  to  $s'$  by the RG (for simplicity, we consider two leads L, R with  $V = \mu_L - \mu_R$  and the case  $E_s = E_{s'}$  here). Energy-conserving transitions from one of the intervals  $d\Lambda$  which are integrated out to the other lead or vice versa can only occur in situation (b).

more details, see Appendix B). The RG equation for  $\Sigma_{ss',s's'} = W_{ss'}$  is identical to the rhs of Eq. (70) for  $s \neq s'$  (note that  $d\Lambda < 0$ , so that the renormalization  $dW_{ss'} > 0$ ),

$$\left(\frac{dW}{d\Lambda}\right)_{ss'} = -2\pi \sum_{pp'=\pm} |g_{\mu\mu'}(p'(\Lambda - |\frac{y}{2}|))_{ss'}|^2 \times \theta_{|y|/2} \theta(py) f_{\Lambda}^p f_{\Lambda-|y|}^{-p}. \quad (71)$$

If the nondiagonal matrix elements of the stationary distribution are zero, the diagonal probabilities  $p_s^{\text{st}} = p_{s's}^{\text{st}}$  follow from the rate equation

$$\sum_{s', s' \neq s} (W_{ss'} p_{s'}^{\text{st}} - W_{s's} p_s^{\text{st}}) = 0, \quad (72)$$

and the stationary current can be written as

$$I_{\text{st}}^{\gamma} = \sum_{ss'} W_{ss'}^{\gamma} p_{s'}^{\text{st}}. \quad (73)$$

The RG for the current rate  $\sum_s W_{ss'}^{\gamma} = \sum_s \Sigma_{ss',s's'}^{\gamma}$  is given by the rhs of Eq. (70) but multiplied with  $2c_{\alpha\alpha'}^{\gamma} = -(\delta_{\gamma\alpha} - \delta_{\gamma\alpha'})$  and summing over  $s$ ,

$$\sum_s \left(\frac{dW^{\gamma}}{d\Lambda}\right)_{ss'} = -2\pi \sum_{spp'} |g_{\mu\mu'}(p'(\Lambda - |\frac{y}{2}|))_{ss'}|^2 \times 2c_{\alpha\alpha'}^{\gamma} \theta_{|y|/2} \theta(py) f_{\Lambda}^p f_{\Lambda-|y|}^{-p}. \quad (74)$$

To calculate the noise at finite frequency  $\Omega$ , we need the frequency dependent vertices  $g_{11',\Omega}$ , arising from the renormalization of the current vertex [Eq. (53)]. They follow from Eq. (62) by replacing the product of the two  $g$  vertices on the rhs by the average  $(1/2)(g_{\Omega}g + gg_{\Omega})$  and

shifting the cutoff  $x_{\sigma}$  by  $\mp\Omega/2$  for the two terms of this average, respectively,

$$(dg_{11',\Omega}/d\Lambda)_{ss'} = -\frac{1}{4} \delta_{\omega_2} \times \left\{ \theta_{\max(T, |x_+ - \Omega/2|, \Gamma)} (g_{12\Omega})_{s\bar{s}} (g_{21'})_{\bar{s}s'} - \theta_{\max(T, |x_- - \Omega/2|, \Gamma)} (g_{21'\Omega})_{s\bar{s}} (g_{12})_{\bar{s}s'} + \theta_{\max(T, |x_+ + \Omega/2|, \Gamma)} (g_{12})_{s\bar{s}} (g_{21'\Omega})_{\bar{s}s'} - \theta_{\max(T, |x_- + \Omega/2|, \Gamma)} (g_{21'})_{s\bar{s}} (g_{12\Omega})_{\bar{s}s'} \right\}. \quad (75)$$

For the Kondo problem without magnetic field, it can then be shown that the diagonal noise follows from  $S_{\Omega}^{\gamma\gamma} = \frac{1}{2} \sum_{ss'} (W_{\Omega}^{\gamma\gamma})_{ss'}$ , where the RG of the noise rate  $\sum_{ss'} (W_{\Omega}^{\gamma\gamma})_{ss'} = \sum_{ss'} (\Sigma_{\Omega}^{\gamma\gamma})_{ss',s's'} + (\Omega \rightarrow -\Omega)$  is given by the rhs of Eq. (70) but multiplied with  $2(c_{\alpha\alpha'}^{\gamma})^2$ , summing over  $s, s'$ , replacing  $g \rightarrow g_{\Omega}$ ,  $y \rightarrow y + \Omega$ , and adding  $\Omega \rightarrow -\Omega$ ,

$$\sum_{ss'} \left(\frac{dW_{\Omega}^{\gamma\gamma}}{d\Lambda}\right)_{ss'} = -4\pi (c_{\alpha\alpha'}^{\gamma})^2 \sum_{ss'pp'} |g_{\mu\mu'}(p'(\Lambda - |\frac{y+\Omega}{2}|))_{ss'}|^2 \times \theta_{|y+\Omega|/2} \theta(p(y+\Omega)) f_{\Lambda}^p f_{\Lambda-|y+\Omega|}^{-p} + (\Omega \rightarrow -\Omega). \quad (76)$$

The noise contribution from  $\Sigma_{\Omega}^{\gamma}$  can be shown to be irrelevant without magnetic field, since  $\Pi(\Omega) = i/\Omega$  in this case (see Appendix B).

## V. TRANSPORT THROUGH SINGLE MOLECULAR MAGNETS

We now apply the formalism to transport through single molecular magnets described by the pseudo-spin- $\frac{1}{2}$  dot Hamiltonian (21) and interaction (22), where  $g_{\mu\mu'} = (1/2)J_{\alpha\alpha'}^i S^i \sigma_{\sigma\sigma'}^i$ . The effective magnetic field  $h$  [differing from the physical magnetic field  $h_z$  used in Eq. (23)] and the exchange interactions are given by Eqs. (24)-(26). Using the form of the interaction in Eq. (66), we obtain a constant, i.e., no contribution to  $L_D$ . Thus, the energies, given by  $E_s = sh/2$ ,  $s = \pm$ , stay invariant. From the vertex RG equation (62), we obtain in leading order

$$\frac{d}{d\Lambda} J_{\alpha\alpha'}^i(\omega) = \frac{1}{4} (\theta_+^i + \theta_-^i) (J_{\alpha\bar{\alpha}}^j J_{\bar{\alpha}\alpha'}^k + J_{\alpha\bar{\alpha}}^k J_{\bar{\alpha}\alpha'}^j), \quad (77)$$

where  $i, j, k$  are all different, and we have defined

$$\theta_{\pm}^z = \theta_{\max(T, |x \pm h|, \Gamma)}, \quad \theta_{\pm}^x = \theta_{\pm}^y = \theta_{\max(T, |x \pm h/2|, \Gamma)}, \quad (78)$$

with  $x = \mu_{\bar{\alpha}} - \mu_{\alpha\alpha'} - \omega$ . From Eq. (71), we obtain for the rates ( $s \neq s'$ )

$$\frac{d}{d\Lambda} W_{ss'} = -(\pi/4) \sum_{ipp'\alpha\alpha'} \delta_{ss'}^i \theta_{\frac{1}{2}y_{\alpha\alpha'}^{is'}} \theta(py_{\alpha\alpha'}^{is'}) \times f_{\Lambda}^p f_{\Lambda-|y_{\alpha\alpha'}^{is'}|}^{-p} J_{\alpha\alpha'}^i [p'(\Lambda - |y_{\alpha\alpha'}^{is'}|)]^2, \quad (79)$$



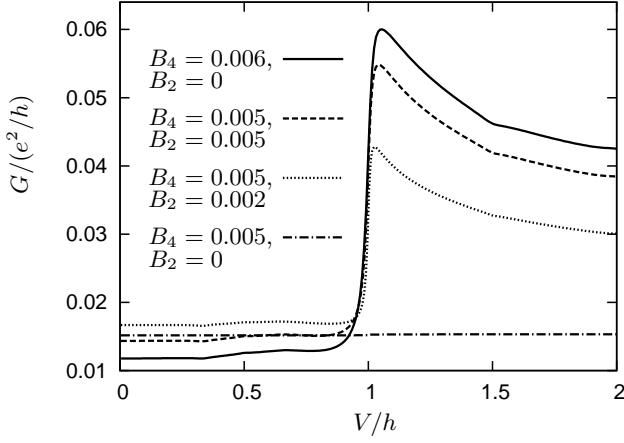


FIG. 4: The differential conductance as function of bias voltage at  $h_z = 10^{-4}$  for different values of  $B_2$  and  $B_4$ . The easy-axis anisotropy of the molecule is  $D = 0.05$  and the coupling to the leads  $J = 0.01$ . We have set  $\Lambda_0 = 1$ .

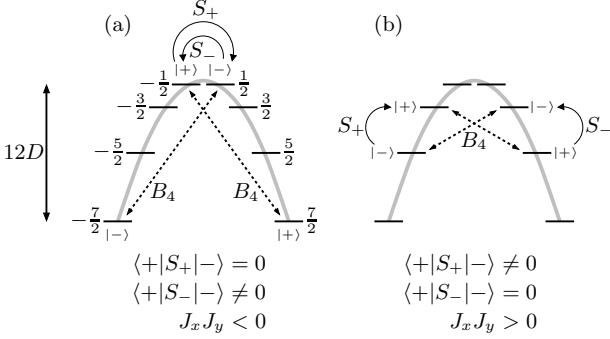


FIG. 5: Energy landscape and coupling of the states of a molecular magnet with  $S = 7/2$ . The longitudinal anisotropy parameter  $D$  determines the height of the parabola  $-DS_z^2$ . The transverse anisotropy constants  $B_2$  and  $B_4$  couple every second or fourth state. For a pure  $B_4$  term, this leads to  $\langle +|S_+|- \rangle$  being zero or finite depending on the size of  $B_4$  since different states form the ground states  $|\pm\rangle$ .

with  $\delta_{ss'}^z = \delta_{ss'}$ ,  $\delta_{ss'}^{x/y} = \delta_{s,-s'}$ , and

$$\begin{aligned} y_{\alpha\alpha'}^{zs'} &= \mu_\alpha - \mu_{\alpha'}, \\ y_{\alpha\alpha'}^{x/y,s'} &= \mu_\alpha - \mu_{\alpha'} - s'h. \end{aligned} \quad (80)$$

The decay rate and the stationary probability follow from  $\Gamma = W_{\uparrow\downarrow} + W_{\downarrow\uparrow}$ ,  $p_{\uparrow}^{\text{st}} = W_{\uparrow\downarrow}/\Gamma$ , and  $p_{\downarrow}^{\text{st}} = W_{\downarrow\uparrow}/\Gamma$ .<sup>23</sup> Current and noise are obtained from Eq. (79) as described at the end of Sec. IV.

Fig. 4 shows the differential conductance as function of the voltage at finite magnetic field for different values of the  $B_2$ - and  $B_4$ -anisotropy constants of a molecular magnet. For small  $B_4$  and  $B_2 = 0$ , we find no Kondo effect for specific spin values  $S = 3/2 + 2m$ ,  $m = 0, 1, \dots$ . In this case, the transverse exchange couplings  $J_{x/y} = J\langle +|S_M^\pm \pm S_M^\mp|- \rangle$  have the property  $J_x J_y < 0$  according to  $\langle +|S_+|- \rangle = 0$  [see Fig. 5(a)]. By increasing either  $B_2$

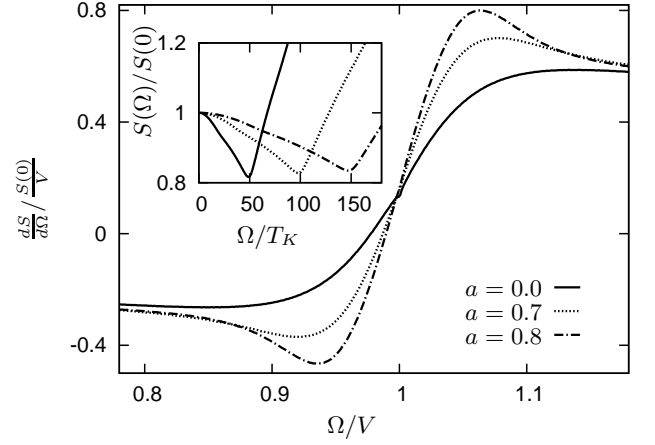


FIG. 6: Derivative of the noise for the isotropic Kondo model without magnetic field at  $V = 50 T_K, a=0$ . The asymmetry of the couplings is described by the asymmetry parameter  $a$ , where  $J_{L,R} = J_0(1 \pm a)$ . Inset: Noise for symmetric couplings and  $V = 50 T_K$  (solid line),  $V = 100 T_K$  (dotted line), and  $V = 150 T_K$  (dash-dotted line), showing a dip at  $\Omega = \pm V$ .

or  $B_4$ , we get  $\langle +|S_+|- \rangle \neq 0$  [see Fig. 5(b)], leading to  $J_x J_y > 0$  with a quantum phase transition at  $J_x J_y = 0$  to a Kondo effect.<sup>14</sup> The latter leads to an increased conductance at  $V = \pm h$  (see Fig. 4).

## VI. NOISE FOR THE ISOTROPIC KONDO MODEL

For  $h = T = 0$  and the isotropic case  $J^i = J$ , we obtain

$$\Gamma = \pi J_{\text{nd}}^2 |_{\Lambda=V} V, \quad (81)$$

$$I_{\text{st}}^L = \frac{3\Gamma}{4}, \quad (82)$$

$$S_{\Omega}^{LL} = \frac{3\pi}{8} \sum_{\pm} J_{\text{nd},\Omega}^2 |_{\Lambda=|V \pm \Omega|} |V \pm \Omega|, \quad (83)$$

with

$$\frac{dJ_{\text{nd},\Omega}}{dl} = \sum_{\pm} \theta_{\max(|V \pm \Omega|, \Gamma)} J_{\text{d}} J_{\text{nd}} \quad (84)$$

in leading order, where  $J_{\text{nd}} = J_{LR} = J_{RL}$  and  $J_{\text{d}} = J_{LL} = J_{RR}$  for a symmetric coupling to the leads. Whereas the decay rate and the current are cut off by the voltage, the noise is cut off by  $|V \pm \Omega|$  which can be tuned to 0 by setting  $\Omega = \pm V$ . As a result, the noise is sensitive to the cutoff  $\Gamma$  of the couplings at these points (see Fig. 6). There is a simple interpretation of the shape of the noise: It can be interpreted in terms of a golden rule expression with two superimposed currents  $\sim J_{\text{nd},\Omega}^2 |_{\Lambda=|V \pm \Omega|} |V \pm \Omega|$  with renormalized couplings (see Fig. 7). For  $\Omega < V$ , the sum of both currents would be independent of  $\Omega$  for bare couplings, but this balancing does not hold for renormalized couplings and a dip

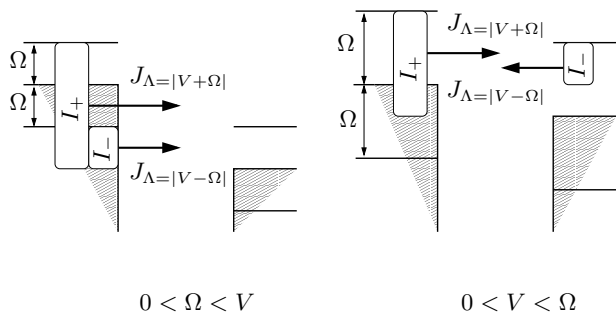


FIG. 7: Left: Interpretation of the finite frequency noise. It corresponds to the sum of two currents with different voltages  $|V \pm \Omega|$  and different renormalized couplings. If both couplings were bare, i.e., not renormalized and therefore equal, the sum would be independent of  $\Omega$  for  $0 < \Omega < V$ . Right: For  $V < \Omega$ , the sum increases with  $\Omega$  even for bare couplings because the absolute value of the currents is important.

evolves (see inset of Fig. 6), whereas for  $\Omega > V$  the noise rises again. The effect of  $\Gamma$  is prominent in the vicinity of  $\Omega = \pm V$ . In Fig. 6, the derivative  $dS(\Omega)/d\Omega$  is shown. The shoulders around  $\Omega = V$  show the logarithmic scaling of the coupling. By tuning the asymmetry, the relaxation rate  $\Gamma$  can be tuned which results in different cutoff heights of the shoulders, leaving the remainder of the noise untouched.

## VII. CONCLUSION AND OUTLOOK

In this work, we have discussed a fundamental model of dissipative quantum mechanics: a local quantum system at fixed particle number coupled via spin or orbital exchange to several electronic reservoirs (the generalization to bosonic reservoirs is straightforward and goes along similar lines). We have proposed that a microscopic derivation of cutoff scales from decay rates should be based on a formulation in terms of the reduced density matrix of the local system, since the decay rates occur naturally by their definition, namely, as the negative imaginary part of the eigenvalues of the kernel determining the time evolution of the reduced density matrix. We have shown that a complete description of decay rates in RG formalism is only possible if one considers the full Keldysh structure, since relaxation and dephasing essentially arise from diagrams connecting the upper with the lower part of the Keldysh contour. Therefore, projecting the RG equation from the very beginning on only one part of the Keldysh contour, one cannot obtain a microscopic description of decay rates. Although energy broadening terms might still lead to a cutoff of the projected RG flow in this case, the physics of relaxation and dephasing is not included. Therefore, our approach provides a consistent nonequilibrium RG formulation which can identify the generation of energy broadening, relaxation, and dephasing at the same time, together with

their influence on the RG flow of the vertices.

Within our formalism, a particular problem arises due to the existence of an eigenvector with zero eigenvalue (the stationary state, which is always present and unique, at least in the absence of symmetry-breaking). It is a nontrivial technical issue to show that this eigenvector does not induce a flow to strong coupling. We have achieved this for a generic quantum dot in the Coulomb blockade regime by analyzing the one-loop RG equations in leading order, including all kinds of boundary vertices determining the dot distribution, the current, and the noise in frequency (Laplace) space. From a pure physical point of view, one does not expect that the presence of a stationary state is correlated to the presence of a strong coupling fixed point, since the former is generic and the latter model-specific. Therefore, we believe that our leading-order analysis will hold in all orders but a general technical proof for this is still lacking. Nevertheless, we have demonstrated within a one-loop formulation that decay rates cut off the RG flow generically. The precise prefactor of the various decay rates cannot be determined by our analytic formulation so far, since certain irrelevant contributions of higher-order terms have been included in the one-loop equations, arising from the  $e^{\pm iL_D t}$ -factors in the definition of the interaction picture [see, e.g., Eq. (41)]. These factors are essential to provide a cutoff scale for the generic case, but lead also to the unwanted effect that certain combinations of decay rates occur which prohibit an unambiguous determination of the correct prefactor. Also here, further developments of nonequilibrium RG are needed to provide generic schemes for problems where the prefactor of the decay rates plays an important role, e.g., for problems with several decay rates differing by many orders of magnitude.

The formulation of this work is useful for problems which stay in the weak-coupling regime with decay rates of the same order of magnitude. In this case, the different prefactors will only lead to very weak logarithmic corrections. We have obtained the physically very natural result that decay rates are only generated when the band width reaches the cutoff scales, defined by voltage, temperature, frequencies, or dot excitations. However, considering the Kondo model, when all these cutoff scales are zero, the only energy scale left is the Kondo temperature  $T_K$ , and we enter the strong-coupling regime for  $\Lambda < T_K$ . An interesting issue for future research is the investigation of the influence of decay rates in the strong-coupling regime. How or whether decay rates will cut off the RG flow also in this case is an open question and has so far not been analyzed. Due to the generic presence of decay rates, we expect them to be important not only for weak-coupling problems. Such developments are highly desirable since no numerical method exists so far which is capable of dealing with the strong-coupling limit of dissipative quantum systems in a nonequilibrium stationary state. Benchmarks for special problems are starting to be developed within the scattering Bethe ansatz

technique,<sup>24</sup> but analytical and numerical methods for generic problems are still missing.

### ACKNOWLEDGMENTS

We thank M. Keil, M. Garst, S. Jakobs, S. Kehrein, J. Paaske, A. Rosch, and T. Novotny for valuable discussions. This work was supported by the VW Foundation and the Forschungszentrum Jülich via the virtual institute IFMIT (T.K., F.R. and H.S.).

### APPENDIX A: DERIVATION OF THE RENORMALIZATION GROUP EQUATIONS

In this appendix, we derive the RG equations (56) and (57) from Fig. 2. As explained in detail in Ref. 1, the  $\Lambda$  dependence of the vertices  $G_{11'}^{p_1 p_1'}$  and the dot Liouvillian  $L_D$  have to be defined in such a way that the total sum of all diagrams stays invariant. This means that the derivatives of these quantities with respect to  $\Lambda$  have to cancel the corresponding RG diagrams of Fig. 2. Using Eq. (32), this gives for the vertex RG from Fig. 2(a)

$$\begin{aligned} -(-i)p_1' \frac{dG_{11'}^{p_1 p_1'}}{d\Lambda} : J_{1+}^{p_1} J_{1'-}^{p_1'} : &= (-i)^2 \int_0 dt p_2 p_2' \\ &\left\{ G_{12,t/2}^{p_1 p_2} G_{2'1',-t/2}^{p_2' p_1'} \frac{d}{d\Lambda} : J_{1+}^{p_1} \overline{J_{2-}^{p_2} J_{2'+}^{p_2'}} J_{1'-}^{p_1'} : \right. \\ &\left. + G_{2'1',t/2}^{p_2' p_1'} G_{12,-t/2}^{p_1 p_2} \frac{d}{d\Lambda} : J_{2'+}^{p_2'} \overline{J_{1'-}^{p_1'} J_{1+}^{p_1}} J_{2-}^{p_2} : \right\}. \end{aligned}$$

Here, the contribution from the upper limit of time integration can be shown to cancel exactly with a corresponding contribution arising from higher order (due to certain correction terms from time ordering; see Ref. 1 for further details), i.e., there is never any divergence. Using

$$: J_{1\eta}^{p_1} J_{1'\eta'}^{p_1'} : = -p_1 p_1' : J_{1'\eta'}^{p_1'} J_{1\eta}^{p_1} : \quad (\text{A1})$$

together with Eq. (42) and omitting the term  $: J_{1+}^{p_1} J_{1'-}^{p_1'} :$  on both sides, we obtain

$$\begin{aligned} \frac{dG_{11'}^{p_1 p_1'}}{d\Lambda} &= i \int_0 dt \left\{ p_2' \frac{d\gamma_{2-,2'+}^{p_2 p_2'}}{d\Lambda} G_{12,t/2}^{p_1 p_2} G_{2'1',-t/2}^{p_2' p_1'} \right. \\ &\left. - p_2 \frac{d\gamma_{2'+,2-}^{p_2' p_2}}{d\Lambda} G_{2'1',t/2}^{p_2' p_1'} G_{12,-t/2}^{p_1 p_2} \right\}. \end{aligned}$$

Inserting Eq. (42) for the contraction and taking matrix elements with respect to the eigenvectors of  $L_D$  gives the RG equation (56) for the vertex.

The RG equation for  $L_D$  is obtained from Fig. 2(b) and reads

$$\begin{aligned} -(-i) \frac{dL_D}{d\Lambda} &= (-i)^2 \int_0 dt p_1' p_2' \\ &G_{11',t/2}^{p_1 p_1'} G_{22',-t/2}^{p_2 p_2'} \frac{d}{d\Lambda} : \overline{J_{1+}^{p_1} J_{1'-}^{p_1'} J_{2+}^{p_2} J_{2'-}^{p_2'}} :. \end{aligned}$$

Using Eqs. (A1) and (42), we get

$$\begin{aligned} \frac{dL_D}{d\Lambda} &= i \int_0 dt p_2 p_2' \\ &\frac{d}{d\Lambda} (\gamma_{1'-,2+}^{p_1 p_2} \gamma_{1+,2'-}^{p_1 p_2'}) G_{11',t/2}^{p_1 p_1'} G_{22',-t/2}^{p_2 p_2'}. \end{aligned}$$

Again, inserting Eq. (42) for the contraction and taking matrix elements with respect to the eigenvectors of  $L_D$ , we obtain the RG equation (57) for the dot Liouvillian.

### APPENDIX B: CURRENT AND NOISE

In order to calculate the probabilities, the current, and the noise from Eqs. (43), (51), and (55), one needs RG equations for the kernels  $\Sigma_\Omega$ ,  $\Sigma_\Omega^\gamma$ , and  $\Sigma_\Omega^{\gamma\gamma'}$ . The perturbation series of  $\Sigma_\Omega$  contains terms of the following structure:

$$\Sigma_\Omega \rightarrow A_\Omega G G \dots G B_\Omega, \quad (\text{B1})$$

with the interaction picture of the two boundary vertices  $A_\Omega$  and  $B_\Omega$  defined by

$$A_{11',\Omega,t}^{pp'} = e^{i\Omega t} e^{iEt} A_{11',\Omega}^{pp'} e^{-iL_D t}, \quad (\text{B2})$$

$$B_{11',\Omega,t}^{pp'} = e^{-i\Omega t} e^{iEt} e^{iL_D t} B_{11',\Omega}^{pp'}, \quad (\text{B3})$$

with  $E = \omega_1 - \omega_1' + \mu_{\alpha_1} - \mu_{\alpha_1}'$ . Initially,  $A_\Omega$  and  $B_\Omega$  are independent of  $\Omega$  and given by the vertex  $G$ , defined in Eq. (33). For the single current kernels  $\Sigma_\Omega^\gamma$  and  $(\Sigma_\Omega^\gamma)^\dagger$ , we have three different types of terms corresponding to whether the current vertex lies at the boundaries or in the middle of a diagram,

$$\begin{aligned} \Sigma_\Omega^\gamma &\rightarrow A_\Omega^{I\gamma} G \dots G B_\Omega \\ &A G \dots G G_\Omega^\gamma G \dots G B_\Omega \\ &A G \dots G \tilde{B}_\Omega^{I\gamma}, \end{aligned} \quad (\text{B4})$$

$$\begin{aligned} \Sigma_\Omega^{\gamma\dagger} &\rightarrow A_\Omega G \dots G B_\Omega^{I\gamma} \\ &A_\Omega G \dots G G_{-\Omega}^\gamma G \dots G B \\ &\tilde{A}_\Omega^{I\gamma} G \dots G B. \end{aligned} \quad (\text{B5})$$

Here,  $X \equiv X_{\Omega=0}$  and all current vertices  $A_\Omega^{I\gamma}$ ,  $\tilde{A}_\Omega^{I\gamma}$ ,  $B_\Omega^{I\gamma}$ ,  $\tilde{B}_\Omega^{I\gamma}$ , and  $G_\Omega^\gamma$  are initially identical to the frequency independent current vertex  $G^\gamma$ , defined in Eq. (49). However, the interaction picture of all these vertices is defined differently and, therefore, they are no longer identical after

renormalization. With  $E = \omega_1 - \omega'_1 + \mu_{\alpha_1} - \mu_{\alpha'_1}$ , the various interaction pictures are defined by

$$A_{11'\Omega,t}^{I\gamma,pp'} = e^{i\Omega t} e^{iEt} A_{11'\Omega}^{I\gamma,pp'} e^{-iL_{\text{D}}t}, \quad (\text{B6})$$

$$B_{11'\Omega,t}^{I\gamma,pp'} = e^{-i\Omega t} e^{iEt} e^{iL_{\text{D}}t} B_{11'\Omega}^{I\gamma,pp'}, \quad (\text{B7})$$

$$G_{11'\Omega,t}^{\gamma,pp'} = e^{i\Omega t} e^{iEt} e^{iL_{\text{D}}t} G_{11'\Omega}^{\gamma,pp'} e^{-iL_{\text{D}}t}, \quad (\text{B8})$$

$$\tilde{A}_{11'\Omega,t}^{I\gamma,pp'} = e^{iEt} \tilde{A}_{11'\Omega}^{I\gamma,pp'} e^{-iL_{\text{D}}t}, \quad (\text{B9})$$

$$\tilde{B}_{11'\Omega,t}^{I\gamma,pp'} = e^{iEt} e^{iL_{\text{D}}t} \tilde{B}_{11'\Omega}^{I\gamma,pp'}. \quad (\text{B10})$$

We note that the two current vertices  $\tilde{A}_{\Omega}^{I\gamma}$  and  $\tilde{B}_{\Omega}^{I\gamma}$  acquire only an implicit frequency dependence via renormalization but not an explicit one from the interaction picture [see Eqs. (B19) and (B20) below].

The RG equations analogous to Eqs. (56) and (57) follow from Fig. 2 by replacing the vertex  $G$  by boundary vertices at the appropriate places,

$$i \frac{d\Sigma_{\Omega}}{d\Lambda} = A_{\Omega} \times B_{\Omega}, \quad (\text{B11})$$

$$i \frac{d\Sigma_{\Omega}^{\gamma}}{d\Lambda} = A_{\Omega}^{I\gamma} \times B_{\Omega} + A \times \tilde{B}_{\Omega}^{I\gamma}, \quad (\text{B12})$$

$$i \frac{d\Sigma_{\Omega}^{\gamma\dagger}}{d\Lambda} = A_{\Omega} \times B_{\Omega}^{I\gamma} + \tilde{A}_{\Omega}^{I\gamma} \times B, \quad (\text{B13})$$

$$i \frac{d\Sigma_{\Omega}^{\gamma\gamma'}}{d\Lambda} = A_{\Omega}^{I\gamma} \times B_{\Omega}^{I\gamma'}, \quad (\text{B14})$$

$$\frac{dA_{\Omega}}{d\Lambda} = A_{\Omega} \cdot G, \quad (\text{B15})$$

$$\frac{dB_{\Omega}}{d\Lambda} = G \cdot B_{\Omega}, \quad (\text{B16})$$

$$\frac{dA_{\Omega}^{I\gamma}}{d\Lambda} = A_{\Omega}^{I\gamma} \cdot G + A \cdot G_{\Omega}^{\gamma}, \quad (\text{B17})$$

$$\frac{dB_{\Omega}^{I\gamma}}{d\Lambda} = G \cdot B_{\Omega}^{I\gamma} + G_{-\Omega}^{\gamma} \cdot B, \quad (\text{B18})$$

$$\frac{d\tilde{A}_{\Omega}^{I\gamma}}{d\Lambda} = \tilde{A}_{\Omega}^{I\gamma} \cdot G + A_{\Omega} \cdot G_{-\Omega}^{\gamma}, \quad (\text{B19})$$

$$\frac{d\tilde{B}_{\Omega}^{I\gamma}}{d\Lambda} = G \cdot \tilde{B}_{\Omega}^{I\gamma} + G_{\Omega}^{\gamma} \cdot B_{\Omega}, \quad (\text{B20})$$

$$\frac{dG_{\Omega}^{\gamma}}{d\Lambda} = G_{\Omega}^{\gamma} \cdot G + G \cdot G_{\Omega}^{\gamma}, \quad (\text{B21})$$

where we have used the abbreviations

$$\begin{aligned} \left( (X \cdot Y)_{11'p_1}^{p_1 p_1'} \right)_{ik} &\equiv i \frac{1}{2} \theta_T \int_0^{\Gamma_j^{-1}} dt \delta_{\omega_2} \text{sign}(\omega_2) \\ &\left\{ (X_{12,t/2}^{p_1 p_2})_{ij} (Y_{21',-t/2}^{p_2 p_1'})_{jk} + \right. \\ &\left. + (X_{21',t/2}^{p_2 p_1'})_{ij} (Y_{12,-t/2}^{p_1 p_2})_{jk} \right\}, \quad (\text{B22}) \end{aligned}$$

$$\begin{aligned} (X \times Y)_{ik} &\equiv i \int_0^{\Gamma_j^{-1}} dt \frac{d}{d\Lambda} (\theta_{\omega_1} \theta_{\omega_2}) p_2 p_2' f_{\omega_1}^{p_2'} f_{\omega_2}^{-p_2} \\ &(X_{12,t/2}^{p_1 p_1'})_{ij} (Y_{21',-t/2}^{p_2 p_2'})_{jk}. \quad (\text{B23}) \end{aligned}$$

Note that we have already used the replacement  $-p f_{\omega_2}^{p_2} \rightarrow \frac{1}{2} - f_{\omega_2} \rightarrow \frac{1}{2} \theta_T \text{sign}(\omega_2)$  in Eq. (B22). As shown in Sec. IV,

this is justified in leading order. We note that for the calculation of the current and noise, given by Eqs. (51) and (55), the boundary vertices  $A_{\Omega}$ ,  $A_{\Omega}^{I\gamma}$ , and  $\tilde{A}_{\Omega}^{I\gamma}$  are only needed by summing over the Keldysh indices,

$$X = \sum_{pp'} X^{pp'} \quad \text{for } X = A_{\Omega}, A_{\Omega}^{I\gamma}, \tilde{A}_{\Omega}^{I\gamma}. \quad (\text{B24})$$

We find that the property (40) is preserved under RG and holds also for the vertices  $A_{\Omega}$  and  $B_{\Omega}$  and for the kernel  $\Sigma_{\Omega}$ , which by using Eq. (59) reads

$$\sum_{pp'} \langle 0 | X_{11'}^{pp'} = 0 \quad \text{for } X = A_{\Omega}, B_{\Omega}, G, \quad (\text{B25})$$

$$\langle 0 | X = 0 \quad \text{for } X = L_{\text{D}}, \Sigma_{\Omega}. \quad (\text{B26})$$

From these properties, we get directly

$$\langle 0 | A_{\Omega}^{pp'} = \langle 0 | G_{\Omega}^{pp'}, \quad (\text{B27})$$

$$\langle 0 | A_{\Omega}^{I\gamma,pp'} = \langle 0 | G_{\Omega}^{\gamma,pp'}, \quad (\text{B28})$$

$$\sum_{pp'} \langle 0 | \tilde{A}_{\Omega}^{I\gamma,pp'} = \sum_{pp'} \langle 0 | G_{\Omega}^{\gamma=0}, \quad (\text{B29})$$

since these quantities fulfill the same RG equation and have the same initial condition.

We now show in leading order that all RG equations are cut off by the decay rate  $\Gamma$ . The proof used in Sec. IV to show that the vertex  $G$  is cut off by  $\Gamma$  can be applied in a similar way to the RG equation (B21) for the vertex  $G_{\Omega}^{\gamma}$ . For the boundary vertices, this proof does not work since the two vertices on the rhs of the RG equations (B15)-(B20) are not equal and the interaction picture of the boundary vertices differs from the one of  $G$  due to the absence of either  $e^{iL_{\text{D}}t}$  (for  $A_{\Omega}$ ,  $A_{\Omega}^{I\gamma}$ , and  $\tilde{A}_{\Omega}^{I\gamma}$ ) to the left or  $e^{-iL_{\text{D}}t}$  (for  $B_{\Omega}$ ,  $B_{\Omega}^{I\gamma}$ , and  $\tilde{B}_{\Omega}^{I\gamma}$ ) to the right. However, we can make use of the property (B25) to show that the eigenvector with eigenvalue zero cannot influence the RG equations in leading order. To show this, we consider as an example an RG equation of the form

$$\begin{aligned} \frac{dX^{pp'}}{d\Lambda} &= (G \cdot X)^{pp'} \\ &= (G^{p\bar{p}} \cdot X^{\bar{p}'p'})^{(1)} + (G^{\bar{p}'p'} \cdot X^{p\bar{p}})^{(2)}, \quad (\text{B30}) \end{aligned}$$

where the two terms on the rhs of (B30) correspond to the two terms on the rhs of Eq. (B22), and the interaction picture of  $X$  is defined according to the boundary vertex  $B$  [for terms contributing to the boundary vertex  $A$ , the analysis is even simpler, since only the form summed over the Keldysh indices is needed; see Eq. (B24)]. Defining

$$\begin{aligned} X &= \sum_{pp'} X^{pp'}, & X_L &= \sum_{pp'} p X^{pp'}, \\ X_R &= \sum_{pp'} p' X^{pp'}, & X_{LR} &= \sum_{pp'} pp' X^{pp'}, \end{aligned}$$

and the same for  $X \rightarrow G$ , we get

$$\frac{dX}{d\Lambda} = (G \cdot X)^{(1)} + (G \cdot X)^{(2)}, \quad (\text{B31})$$

$$\frac{dX_L}{d\Lambda} = (G_L \cdot X)^{(1)} + (G \cdot X_L)^{(2)}, \quad (\text{B32})$$

$$\frac{dX_R}{d\Lambda} = (G \cdot X_R)^{(1)} + (G_R \cdot X)^{(2)}, \quad (\text{B33})$$

$$\frac{dX_{LR}}{d\Lambda} = (G_R \cdot X_L)^{(1)} + (G_L \cdot X_R)^{(2)}. \quad (\text{B34})$$

We now consider the contribution when the two eigenvectors  $i = j = 0$  in Eq. (B22) have zero eigenvalue, i.e.,  $\lambda_i = \lambda_j = 0$  (note that the eigenvalue  $\lambda_k$  cannot lead to any cutoff since the factor  $e^{-iL_D t}$  to the right is missing in the definition of the interaction picture of  $X$ ). Due to  $\langle 0|G = \langle 0|X = 0$ , we see that this term does not lead to any contribution in Eqs. (B31)-(B33). Only for (B34) can the case  $i = j = 0$  contribute and no cutoff from a decay rate occurs. However, since the vertices  $G_L$ ,  $G_R$ ,  $X_L$ , and  $X_R$  are cut off by the decay rate, this term leads only to a logarithmic correction to  $X_{LR}$  which is integrable and subleading (note that frequencies enter the argument of the logarithm, making this term finite when integrated over the frequencies). Therefore, we see that we do not have to consider the eigenvalue zero in leading order (we expect that a similar proof holds in all orders but this cannot be seen from one-loop RG equations).

A similar analysis can be performed for all terms of the RG equations (B15)-(B20). With this result, we can replace  $L_D \rightarrow L_D^{\text{rel}} = [H_D, \cdot]$  on the rhs of Eq. (B22) and introduce an overall cutoff factor  $\theta_\Gamma$ ,

$$(X \cdot Y)_{11'}^{p_1 p_1'} \equiv i \frac{1}{2} \theta_\Gamma \theta_T \int_0 dt \delta_{\omega_2} \text{sign}(\omega_2) \left\{ X_{12, t/2}^{p_1 p_2} Y_{21', -t/2}^{p_2' p_1'} + X_{21', t/2}^{p_2' p_1'} Y_{12, -t/2}^{p_1 p_2} \right\}_{L_D \rightarrow L_D^{\text{rel}}}. \quad (\text{B35})$$

For Eq. (B23), we use the same but neglect the decay rates on the rhs because this does not cause any divergence (the resulting  $\delta$ - and principal value integrals are convergent),

$$X \times Y \equiv i \int_0 dt e^{-t0^+} \frac{d}{d\Lambda} (\theta_{\omega_1} \theta_{\omega_2}) p_2 p_2' f_{\omega_1}^{p_2'} f_{\omega_2}^{-p_2} \times X_{12, t/2}^{p_1 p_1'} Y_{21', -t/2}^{p_2 p_2'} \Big|_{L_D \rightarrow L_D^{\text{rel}}}. \quad (\text{B36})$$

In the next step, we show that above all cutoff scales, the current vertices preserve their initial form (49) together with Eqs. (33) and (34). To prove this, we evaluate (B35) for  $\Lambda$  larger than all cutoff scales and get

$$(X \cdot Y)_{11'}^{p_1 p_1'} \equiv \frac{1}{\Lambda} \left( X_{12}^{p_1 p_2} Y_{21'}^{p_2' p_1'} - X_{21'}^{p_2' p_1'} Y_{12}^{p_1 p_2} \right). \quad (\text{B37})$$

Inserting this form in the RG equations (B15)-(B21), we find that all vertices are independent of  $\Omega$  and we get

$A = B = G$  and  $A^{I\gamma} = \tilde{A}^{I\gamma} = B^{I\gamma} = \tilde{B}^{I\gamma} = G^\gamma$ . Furthermore, inserting the initial form (49) together with Eq. (33) for the vertex  $G_{11'}^{\gamma, pp'} = -\frac{1}{2}(\delta_{\alpha_1 \gamma} - \delta_{\alpha_1' \gamma}) p' \delta_{pp'}$  on the rhs of the RG equation (B21), we find

$$\frac{dG_{11'}^{\gamma, p_1 p_1'}}{d\Lambda} = -\frac{1}{2} \frac{1}{\Lambda} \left\{ p_1 (\delta_{\alpha_1 \gamma} - \delta_{\alpha_2 \gamma}) [G_{12}^{p_1 p_1}, G_{21'}^{p_1' p_1'}] - p_1' (\delta_{\alpha_2 \gamma} - \delta_{\alpha_1' \gamma}) [G_{21'}^{p_1' p_1'}, G_{12}^{p_1 p_1}] \right\}.$$

Using the initial form (34) of the vertex  $G^{pp}$ , we find  $[G^{++}, G^{--}] = 0$  and we get

$$\begin{aligned} \frac{dG_{11'}^{\gamma, p_1 p_1'}}{d\Lambda} &= -\frac{1}{2} (\delta_{\alpha_1 \gamma} - \delta_{\alpha_1' \gamma}) p_1 \delta_{p_1 p_1'} \frac{1}{\Lambda} \left[ G_{12}^{p_1 p_1}, G_{21'}^{p_1' p_1'} \right] \\ &= \frac{d}{d\Lambda} \left\{ -\frac{1}{2} (\delta_{\alpha_1 \gamma} - \delta_{\alpha_1' \gamma}) p_1 \delta_{p_1 p_1'} G_{11'}^{p_1 p_1'} \right\}, \end{aligned}$$

where we have used the RG equation (61) above all cutoff scales in the last line. This shows that the initial form (49) of the current vertex is preserved in leading order. Therefore, for all vertices  $X \equiv G, A^I, B^I, \tilde{A}^I, \tilde{B}^I$ , we use the form

$$X_{11' \Omega}^{\gamma, pp'} = c_{\alpha_1 \alpha_1'}^\gamma p' X_{11' \Omega}^{pp'}, \quad (\text{B38})$$

also below the cutoff scales, together with

$$X_{11' \Omega}^{pp'} = \delta_{pp'} X_{11' \Omega}^{pp} \quad (\text{B39})$$

for all  $X \equiv G, A, B, A^I, B^I, \tilde{A}^I, \tilde{B}^I$ . Inserting the form (B38) for the current vertices into the RG equations (B17)-(B21) and neglecting all terms on the rhs which do not preserve this form (and become zero above all cutoff scales), we find the same RG equations for the  $\gamma$ -independent vertices  $A_\Omega^I, B_\Omega^I, \tilde{A}_\Omega^I, \tilde{B}_\Omega^I, G_\Omega$  but with an additional factor  $\frac{1}{2}$  appearing on the rhs of the RG equations,

$$\frac{dA_\Omega^I}{d\Lambda} = \frac{1}{2} \{ A_\Omega^I \cdot G + A \cdot G_\Omega \}, \quad (\text{B40})$$

$$\frac{dB_\Omega^I}{d\Lambda} = \frac{1}{2} \{ G \cdot B_\Omega^I + G_{-\Omega} \cdot B \}, \quad (\text{B41})$$

$$\frac{d\tilde{A}_\Omega^I}{d\Lambda} = \frac{1}{2} \{ \tilde{A}_\Omega^I \cdot G + A_\Omega \cdot G_{-\Omega} \}, \quad (\text{B42})$$

$$\frac{d\tilde{B}_\Omega^I}{d\Lambda} = \frac{1}{2} \{ G \cdot \tilde{B}_\Omega^I + G_\Omega \cdot B_\Omega \}, \quad (\text{B43})$$

$$\frac{dG_\Omega}{d\Lambda} = \frac{1}{2} \{ G_\Omega \cdot G + G \cdot G_\Omega \}. \quad (\text{B44})$$

Using Eq. (B35) in the RG equations (B15), (B16), and (B40)-(B44), one can easily prove the following useful relationships between the vertices [note that the form  $L_D^{\text{rel}} = [H_D, \cdot]$  implies  $L_D^{\text{rel}} = (L_D^{\text{rel}})^\dagger$ ]:

$$G_\Omega^\dagger = G_{-\Omega}, \quad (\text{B45})$$

$$A_\Omega^\dagger = B_\Omega, \quad (\text{B46})$$

$$A_\Omega^{I\dagger} = B_\Omega^I, \quad (\text{B47})$$

$$(\tilde{A}_\Omega^I)^\dagger = \tilde{B}_\Omega^I. \quad (\text{B48})$$

Furthermore, we get the following properties for the matrix representations of the vertices:

$$\sum_p \sum_s (X_{11'\Omega}^{pp})_{ss,\dots} = 0, \quad (\text{B49})$$

$$(X_{11'\Omega}^{pp})_{s_1 s'_1, s_2 s'_2} = -(X_{1'1, -\Omega}^{-p, -p})_{s'_1 s_1, s'_2 s_2}^* \quad (\text{B50})$$

for all vertices  $X = G, A, B, A^I, B^I, \tilde{A}^I, \tilde{B}^I$ .

The RG equation (B44) for the vertex  $G_\Omega$  becomes especially simple. If one uses Eqs. (B35) and (B39) and  $L_D^{\text{rel}} = [H_D, \cdot]$ , one finds that the initial form

$$G_{11'\Omega}^{++} = g_{11'\Omega}, \quad G_{11'\Omega}^{--} = - \cdot g_{11'\Omega} \quad (\text{B51})$$

is preserved under renormalization. Therefore, one can project this RG equation exactly on the upper Keldysh contour and obtain

$$\frac{dg_\Omega}{d\Lambda} = \frac{1}{2} \{g_\Omega \cdot g + g \cdot g_\Omega\}, \quad (\text{B52})$$

where in analogy to Eqs. (B35) and (B8), we have defined

$$(x \cdot y)_{11'} \equiv i \frac{1}{2} \theta_T \theta_T \int_0 dt \delta_{\omega_2} \text{sign}(\omega_2) \{x_{12, t/2} y_{21', -t/2} + x_{21', t/2} y_{12, -t/2}\} \quad (\text{B53})$$

and

$$g_{11'\Omega, t} = e^{i\Omega t} e^{iEt} e^{iH_D t} g_{11'\Omega} e^{-iH_D t}, \quad (\text{B54})$$

with  $E = \omega_1 - \omega'_1 + \mu_{\alpha_1} - \mu_{\alpha'_1}$ . Evaluating Eq. (B52) gives Eq. (75) of Sec. IV. We note that this projection on the upper Keldysh contour is not exactly possible for the boundary vertices since the interaction picture is defined differently. Whereas for the vertex  $G_\Omega^{pp}$  we can use

$$G_{11'\Omega, t}^{++} = g_{11'\Omega, t}, \quad G_{11'\Omega, t}^{--} = - \cdot g_{11'\Omega, t},$$

a similar equation does not hold for the boundary vertices. Using Eqs. (B45) and (B51), we get

$$g_{11'\Omega}^\dagger = g_{1'1, -\Omega}. \quad (\text{B55})$$

Finally, we note that for not more than two reservoirs, the generation of double-current vertices must not be considered, since they can be shown to be irrelevant, i.e., they are not generated above all cutoff scales, at least if the trace over the dot states and the sum over the Keldysh indices are taken [which is the quantity entering the noise formula (55)]. To prove this, we use the leading order form (B37) above all cutoff scales and get for the RG of double current vertices  $G^{\gamma\gamma'}$

$$\sum_{p_1 p'_1} \text{Tr}_D \frac{dG_{11'}^{\gamma\gamma', p_1 p'_1}}{d\Lambda} = \frac{1}{\Lambda} \sum_{p_1 p_2 p'_1 p'_2} \text{Tr}_D \left\{ G_{12}^{\gamma, p_1 p_2} G_{21'}^{\gamma', p'_2 p'_1} - G_{21'}^{\gamma, p'_2 p'_1} G_{12}^{\gamma', p_1 p_2} \right\}.$$

Inserting the form (B38), (B39), and (B51) for the current vertex, we get after some straightforward manipulations

$$\sum_{p_1 p'_1} \text{Tr}_D \frac{dG_{11'}^{\gamma\gamma', p_1 p'_1}}{d\Lambda} = \frac{1}{4\Lambda} \{(\delta_{\alpha_1 \gamma} - \delta_{\alpha_2 \gamma})(\delta_{\alpha_2 \gamma'} - \delta_{\alpha'_1 \gamma'}) - (\delta_{\alpha_1 \gamma'} - \delta_{\alpha_2 \gamma'}) (\delta_{\alpha_2 \gamma} - \delta_{\alpha'_1 \gamma'})\} \text{Tr}_D (g_{12} g_{21'} + g_{21'} g_{12}).$$

For two reservoirs, the rhs of this equation can easily be seen to be zero either for  $\gamma = \gamma'$  or  $\gamma \neq \gamma'$ .

The complicated set of RG equations simplifies considerably if one considers a problem where the dot distribution is diagonal  $(p_\Omega)_{ss'} = \delta_{ss'} (p_\Omega)_s$  and where the dot eigenstates  $|s\rangle$  do not renormalize (however, the dot energies  $E_s$  can renormalize). This is, e.g., the case for the fully anisotropic Kondo model under consideration in this work, given by Eqs. (21)-(26), due to rotational invariance around the  $z$  axis. In this case, we need for the dot distribution (43), the current (51), and the noise (55) only the matrix elements  $X_{ss, s's'}$  ( $X = \Sigma_\Omega, \Sigma_\Omega^\gamma, \Sigma_\Omega^{\gamma\dagger}, \Sigma_\Omega^{\gamma\gamma'}$ ) for the kernels. As a consequence, we see from (B11)-(B14) and (B38) that only the components  $X_{ss, \dots}$  ( $X = A_\Omega, A_\Omega^I, \tilde{A}_\Omega^I$ ) and  $X_{\dots, ss}$  ( $X = B_\Omega, B_\Omega^I, \tilde{B}_\Omega^I$ ) of the boundary vertices are needed. Using the matrix representation of  $L_D^{\text{rel}} = [H_D, \cdot]$  [see Eq. (36)],

$$(L_D^{\text{rel}})_{s_1 s'_1, s_2 s'_2} = (E_{s_1} - E_{s'_1}) \delta_{s_1 s_2} \delta_{s'_1 s'_2}, \quad (\text{B56})$$

we find  $(L_D^{\text{rel}})_{ss, s's'} = 0$  and we get

$$(A_\Omega)_{ss, \dots} = (A_\Omega^I)_{ss, \dots} = (G_\Omega)_{ss, \dots}, \quad (\text{B57})$$

$$(B_\Omega)_{\dots, ss} = (B_\Omega^I)_{\dots, ss} = (G_\Omega)_{\dots, ss}, \quad (\text{B58})$$

since the interaction pictures and the RG equations are the same for the various quantities. For the boundary vertices  $\tilde{A}_\Omega$  and  $\tilde{B}_\Omega$ , we get this property only after summing over the states and the Keldysh indices, since otherwise the second term on the rhs of Eqs. (B42) and (B43) contributes and leads to different renormalizations. Analogous to Eq. (B29), we get

$$\sum_{pp's} (\tilde{A}_\Omega^{I, pp'})_{ss, \dots} = \sum_{pp's} (G_{\Omega=0}^{pp'})_{ss, \dots}, \quad (\text{B59})$$

$$\sum_{pp's} (\tilde{B}_\Omega^{I, pp'})_{\dots, ss} = \sum_{pp's} (G_{\Omega=0}^{pp'})_{\dots, ss}. \quad (\text{B60})$$

Therefore, we need only the RG equation (B52) for the vertex  $g_\Omega$  and we can easily evaluate Eqs. (B11)-(B14) by using Eqs. (B36), (B38), (B51), and (19),

$$\frac{d(\Sigma_\Omega)_{ss, s's'}}{d\Lambda} = -i \frac{d}{d\Lambda} (\theta_\omega \theta_{\omega'}) f_\omega^- f_{\omega'}^+ \times \left\{ \frac{|g_{\mu\mu'}(\omega, \omega')_{ss'}|^2}{\Omega + \omega - \omega' + y + i\eta} - (\Omega \rightarrow -\Omega)^* \right\}, \quad (\text{B61})$$

for  $s \neq s'$ , and

$$\sum_s \frac{d(\Sigma_\Omega^\gamma)_{ss,s's'}}{d\Lambda} = -i 2 c_{\alpha\alpha'}^\gamma \frac{d}{d\Lambda} (\theta_\omega \theta_{\omega'}) f_\omega^- f_{\omega'}^+ \times \sum_s \left\{ \frac{|g_{\mu\mu'}\Omega(\omega, \omega')_{ss'}|^2}{\Omega + \omega - \omega' + y + i\eta} - (\Omega \rightarrow -\Omega)^* \right\}, \quad (\text{B62})$$

$$\sum_s \frac{d(\Sigma_\Omega^{\gamma\gamma'})_{ss,s's'}}{d\Lambda} = -i 2 c_{\alpha\alpha'}^\gamma c_{\alpha\alpha'}^{\gamma'} \frac{d}{d\Lambda} (\theta_\omega \theta_{\omega'}) f_\omega^- f_{\omega'}^+ \times \sum_s \left\{ \frac{|g_{\mu\mu'}\Omega(\omega, \omega')_{ss'}|^2}{\Omega + \omega - \omega' + y + i\eta} - (\Omega \rightarrow -\Omega)^* \right\}, \quad (\text{B63})$$

$$\sum_s \frac{d(\Sigma_\Omega^{\gamma\dagger})_{ss,s's'}}{d\Lambda} = \sum_s \frac{d(\Sigma_{\Omega=0}^\gamma)_{ss,s's'}}{d\Lambda}, \quad (\text{B64})$$

with  $y = \mu_\alpha - \mu_{\alpha'} + E_s - E_{s'}$ . For  $\Omega = 0$ , Eq. (B61) leads to Eq. (71) and Eq. (B62) to Eq. (74) of Sec. IV, giving the stationary dot distribution and the stationary current [the time-dependence of the dot distribution and the current for an arbitrary initial state can also be calculated from Eqs. (43) and (51)]. The calculation for the noise simplifies considerably if the above matrix elements do not depend on  $s$  (which is the case, e.g., for the isotropic Kondo model in the absence of a magnetic field due to spin symmetry). In this case, we can average over  $s$  and get from (B64) and (B26) the explicit formulas

$$(\Sigma_\Omega^\dagger)_{ss,s's'} = \frac{1}{2} \sum_s (\Sigma_\Omega^\dagger)_{ss,s's'} = 0, \quad (\text{B65})$$

$$\begin{aligned} (\Sigma_\Omega^{\gamma\dagger})_{ss,s's'} &= \frac{1}{2} \sum_s (\Sigma_\Omega^{\gamma\dagger})_{ss,s's'} \\ &= \frac{1}{2} \sum_s (\Sigma_{\Omega=0}^\gamma)_{ss,s's'}. \end{aligned} \quad (\text{B66})$$

Therefore, we get  $(\Pi_\Omega)_{ss,s's'} = i/\Omega$  from Eq. (43), and using Eqs. (27) and (55), we obtain for the diagonal noise [the nondiagonal one follows from Eq. (29)] for  $\Omega \neq 0$

$$\begin{aligned} S_\Omega^{\gamma\gamma} &= \frac{1}{Z} \sum_{ss'} (\Sigma_\Omega^{\gamma\gamma} + \Sigma_{-\Omega}^{\gamma\gamma})_{ss,s's'} \\ &+ \frac{1}{Z} \frac{i}{2\Omega} \left\{ \sum_{ss'} (\Sigma_\Omega^\gamma - \Sigma_{-\Omega}^\gamma)_{ss,s's'} \right\} \left\{ \sum_{ss'} (\Sigma_{\Omega=0}^\gamma)_{ss,s's'} \right\}, \end{aligned} \quad (\text{B67})$$

where we have used  $p_s^{\text{st}} = 1/Z$  with  $Z$  denoting the number of dot states. Using Eq. (B63), we get directly the RG equation (76) of Sec. IV for  $\sum_{ss'} (\Sigma_\Omega^{\gamma\gamma} + \Sigma_{-\Omega}^{\gamma\gamma})_{ss,s's'}$ . Concerning the second term on the rhs of Eq. (B67), we use Eq. (B62) and interchange  $\mu \leftrightarrow \mu'$ ,  $\omega \leftrightarrow \omega'$  and  $s \leftrightarrow s'$  in the second term on the rhs of this equation. With the help of Eq. (B55), this gives the result

$$\begin{aligned} \frac{d}{d\Lambda} \sum_{ss'} (\Sigma_\Omega^\gamma - \Sigma_{-\Omega}^\gamma)_{ss,s's'} &= \\ &= -4i c_{\alpha\alpha'}^\gamma \frac{d}{d\Lambda} (\theta_\omega \theta_{\omega'}) (f_{\omega'} - f_\omega) \\ &\times \text{P} \left( \frac{1}{\Omega + \omega - \omega' + \mu_\alpha - \mu_{\alpha'}} \right) \sum_{ss'} |g_{\mu\mu'}\Omega(\omega, \omega')_{ss'}|^2. \end{aligned}$$

Performing the integrals over  $\omega$  and  $\omega'$  by neglecting the frequency-dependence of  $g_{\mu\mu'}\Omega(\omega, \omega')$ , one finds that this term leads to a contribution of the order  $\Gamma \times \text{O}(\frac{V}{\Lambda_0}, \frac{\Omega}{\Lambda_0})$ . Therefore, it is irrelevant and is left out within our leading order analysis.

- 
- <sup>1</sup> H. Schoeller, in *Low-Dimensional Systems*, ed. T. Brandes, Lect. Notes Phys. (Springer, Berlin/Heidelberg, 2000), p. 137.
- <sup>2</sup> H. Schoeller and J. König, Phys. Rev. Lett. **84**, 3686 (2000).
- <sup>3</sup> M. Keil and H. Schoeller, Phys. Rev. **B63**, 180302(R) (2001).
- <sup>4</sup> P. Coleman, C. Hooley, and O. Parcollet, Phys. Rev. Lett. **86**, 4088 (2001).
- <sup>5</sup> A. Rosch, J. Kroha, and P. Wölfle, Phys. Rev. Lett. **87**, 156802 (2001); A. Rosch, J. Paaske, J. Kroha, and P. Wölfle, Phys. Rev. Lett. **90**, 076804 (2003).
- <sup>6</sup> A. Mitra, S. Takei, Y.B. Kim, and A.J. Millis, Phys. Rev. Lett. **97**, 236808 (2006).
- <sup>7</sup> S. Kehrein, Phys. Rev. Lett. **95**, 056602 (2005).
- <sup>8</sup> S. G. Jakobs, V. Meden, and H. Schoeller, Phys. Rev. Lett. **99**, 150603 (2007).
- <sup>9</sup> R. Gezzi, Th. Pruschke, and V. Meden, Phys. Rev. B **75**, 045324 (2007).
- <sup>10</sup> A. Kaminski, Yu. V. Nazarov, and L. I. Glazman, Phys. Rev. B **62**, 8154 (2000).
- <sup>11</sup> P. W. Anderson, J. Phys. **C3**, 2436 (1970); F. D. M. Haldane, Phys. Rev. Lett. **40**, 416 (1978); A. C. Hewson, *The Kondo Problem to Heavy Fermions* (Cambridge University Press, Cambridge, 1997).
- <sup>12</sup> L. I. Glazman and M. E. Raikh, Pis'ma Zh. Eksp. Teor. Fiz. **47**, 378 (1988) [JETP Lett. **47**, 452 (1988)]; T. K. Ng and P. A. Lee, Phys. Rev. Lett. **61**, 1768 (1988).
- <sup>13</sup> D. Goldhaber-Gordon *et al.*, Nature **391**, 156 (1998); S. M. Cronenwett *et al.*, Science **281**, 540 (1998); F. Simmel, R. H. Blick, J. P. Kotthaus, W. Wegscheider, and M. Bichler, Phys. Rev. Lett. **83**, 804 (1999).
- <sup>14</sup> C. Romeike, M.R. Wegewijs, W. Hofstetter, and H. Schoeller, Phys. Rev. Lett. **96**, 196601 (2006).
- <sup>15</sup> C. Romeike, M. R. Wegewijs, W. Hofstetter, H. Schoeller, Phys. Rev. Lett. **97**, 206601 (2006).
- <sup>16</sup> A. Schiller and S. Hershfield, Phys. Rev. B **58**, 14978 (1998).
- <sup>17</sup> J. R. Schrieffer and P. A. Wolff, Phys. Rev. **149**, 491 (1966).
- <sup>18</sup> J. Koch, M. E. Raikh, and F. von Oppen, Phys. Rev. Lett. **96**, 056803 (2006).

- <sup>19</sup> D. Boese, W. Hofstetter, and H. Schoeller, Phys. Rev. B **64**, 125309 (2001).
- <sup>20</sup> M. Braun, J. König, and J. Martinek, Phys. Rev. B **70**, 195345 (2004).
- <sup>21</sup> M. Braun, J. König, and J. Martinek, Phys. Rev. B **74**, 075328 (2006).
- <sup>22</sup> If  $\Gamma_j = 0$ , one can show that the contribution from the upper limit of integration cancels exactly with a corresponding contribution from higher order, i.e., there is never any divergence.
- <sup>23</sup> In the fully anisotropic Kondo model, there are three different decay rates with similar scale. We have taken the  $1/T_1$ -rate here.
- <sup>24</sup> P. Mehta and N. Andrei, Phys. Rev. Lett. **96**, 216802 (2006).